Cratering Characteristics of the Europa Kinetic Ice Penetrator

Mariah L. Danner

A thesis

submitted in partial fulfillment of the

requirements for the degree of

Master of Science

University of Washington

2018

Reading Committee:

Robert Winglee, Chair

Erika Harnett

Michael McCarthy

Program Authorized to Offer Degree:

Earth and Space Sciences

University of Washington

Abstract

Cratering Characteristics of the Europa Kinetic Ice Penetrator

Mariah L. Danner

Chair of the Supervisory Committee:
Professor Robert Winglee
Earth and Space Sciences

This thesis further develops the Europa Kinetic Ice Penetrator (EKIP) landing technique for airless bodies, as well as characterizes the effect EKIP would have on Europa's surface. Damage to the extremophile Planococcus Halocryophilus OR1 (PHOR1) during a laboratory hypervelocity impact test was studied the effect of rapid application of pressure to microbes frozen in ice. Significant die-off occurred, however PHOR1 microbes survived a 2.2km/s impact. Field testing the second-stage deployment, as well as to characterize crater morphology of the EKIP system was conducted. With low impact velocities, penetrators consistently had deeper, narrower craters than natural impactors (rocks), and showed less radial and sub-impactor compression. This, and future crater data into harder substrates, will create a cratering hardness curve for this design impactor into airless bodies. This curve, used with the eventual in situ craters, can be used to constrain the hardness and other physical properties of the surface of icy-bodies.

TABLE OF CONTENTS

LIST OF FIGURES

LIST OF TABLES

Chapter 1. INTRODUCTION

1.1 BACKGROUND

The Galilean moons of Jupiter have recently been the focus of interplanetary science missions, with continued interest in the icy moon Europa as an important astrobiology target. Of particular interest to its subsurface ocean, which may sustain life. Research into the chemistry and geology of both the icy shell and oceanic subsurface continue (see Appendix A). Previous missions, such as Rosetta's Philae lander and its unsuccessful anchoring to cometary ice, exemplify our lack of in-depth knowledge into the dynamics of extra-planetary ice.

The next mission, the Europa Clipper, is being designed to "clip", or side-swipe, Europa as the satellite navigates through the Jovian system's complex orbits and radiation bands. Due to congressional mandate, a lander will launch from the Europa Clipper to explore Europa's surface. Two main lander designs are underway; a traditional lander designed by NASA's Jet Propulsion Laboratory (JPL), and the Europa Kinetic Ice Penetrator, EKIP, led by the University of Washington, in collaboration with NASA Ames. (Winglee et al., 2018).

The EKIP concept is designed around the process/theory of 'cryo-braking', a technique to slow the lander down in a near-zero atmosphere environment using a two stage system. Cryo-braking uses the transfer of kinetic energy/momentum from a kinetic impact to form a channelized debris plume to an impact-lander. As shown in Figure 1.2 the Europa Kinetic Ice Penetrator will separate from the Europa Clipper, departing the satellite with a small Delta V relative to the spacecraft but with a speed of roughly 4 km/s relative to Europa's orbital speed. With the velocity imparted from the Clipper the lander will approach the Europan surface, separating into two distinct stages. Once separated, the first stage will continue towards the

surface while the second stage deploys a mechanical chute. The penetrator will impact the ice, creating the channelized ice plume necessary for cryo-braking. As the second stage interacts with the ice plume, the second stage will decelerate to a velocity the onboard instrumentation can withstand. The momentum transfer will be enough to slow, but not stop, the second stage, allowing for a low-velocity impact of the second stage. Due to the braking being caused by relative velocity differences of the two stages instead of fuel, contamination of Europa's surface is less likely.

This thesis will focus on research done on the effects of the EKIP landing system would have on Europa's surface, namely the craters caused by the impactor system, to develop an empirical theory for engineered impacts into extra-planetary ice. It will be possible to apply this theory to better understand the dynamic continuum of planetary ice in a way that is difficult using traditional methods. The effects of impacts on possible microbial life will also be addressed.

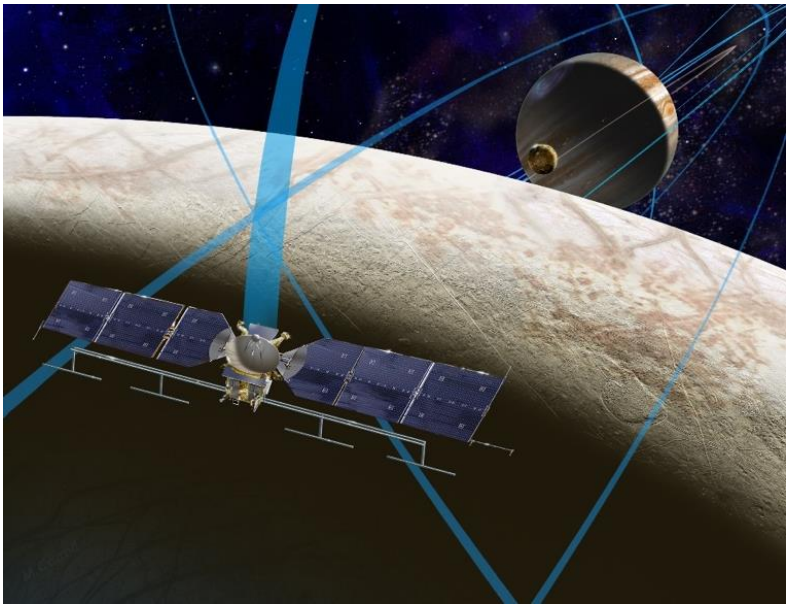

Figure 1.1. Artist rendition of Europa Clipper, image credit: *NASA/JPL-Caltech*

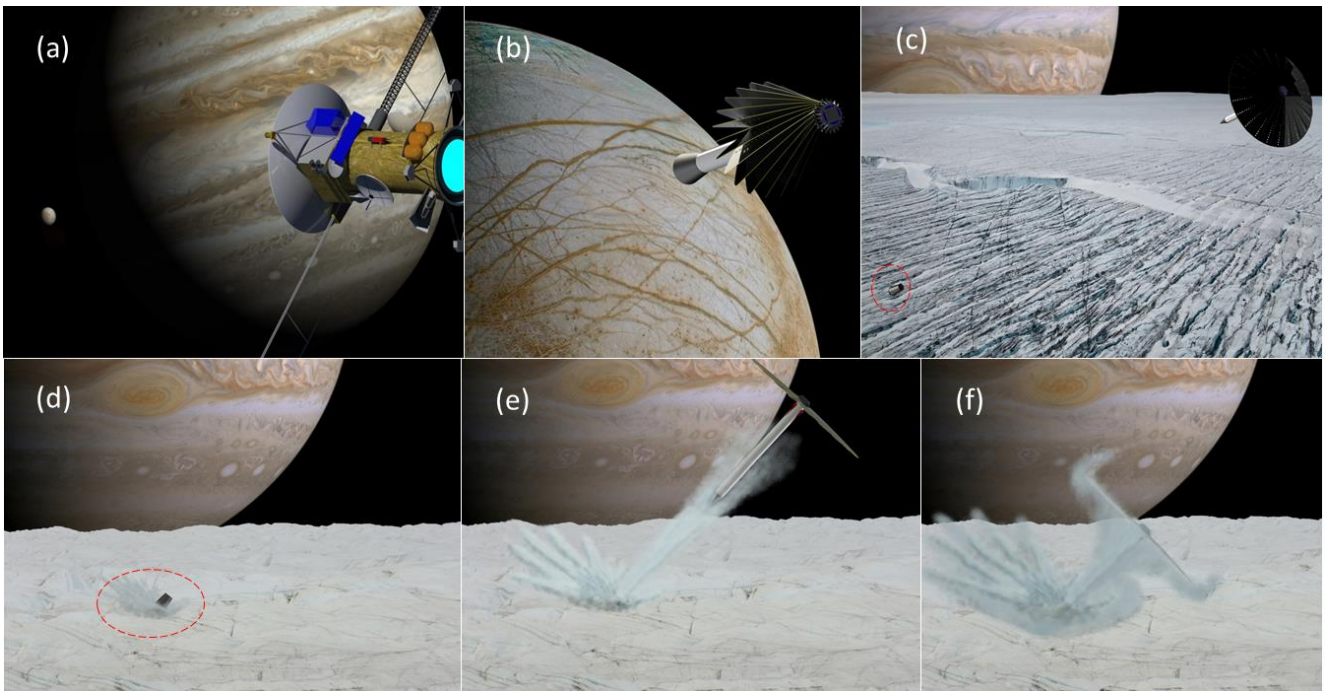

Figure 1.2. Artist rendition of the Europa Kinetic Ice Penetrator departing from the Europa Clipper. After separation from the Clipper, the lander separates into two stages; As the first stage impacts the surface (d), it creates a plume that interacts with and decelerates the second stage (e and f).

1.2 Previous Work

1.2.1 *The "Grave-Digger" Asteroid Penetrator*

The Europa Kinetic Ice Penetrator derived from a previously funded project, the "Grave-Diggers", or the asteroid penetrators also being developed at the University of Washington.

This system of asteroid sampling utilizes impactors contained on a satellite, which once launched will impact a given asteroid. As shown in Figure 1.3, the penetrator body consists of a hardened nose cone, with a hollow bore for which the impacted substrate flows. Once the sample

fills an interior sample return canister, a tether is able to retrieve the sample from the asteroid. Preliminary testing of the Grave-Digger system created a rock core, shown in Figure 1.4. When the penetrator impacted sandstone at a velocity nearing Mach 2, the sandstone flowed into the sample bore, but stagnated within the penetrator body. (Truitt 2016). Redesign of the interior sample return canister, including a shock absorbing spring, enabled rock sample to flow into the canister and eject upon impact (Winglee et al, 2017). The ejected sample retained the stratigraphy of the impacted rock, along with the macro-biology in the overlaying soil.

Nose cone and experimental designs from the Grave-Digger system have been modified for the EKIP landing system, utilizing the penetrator to break up the ice to eject a transient atmosphere that can be used to provide passive braking for a following payload.

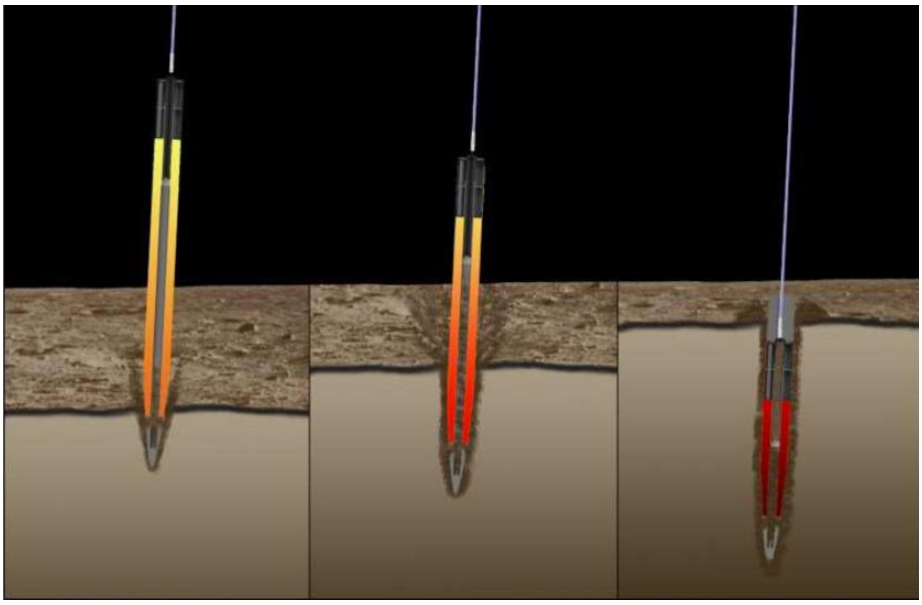

Figure 1.3. Artistic rendition of asteroid penetrator system. Hollow bore up the center of the impactor allows for rock flow into a sample chimney. Image courtesy of Chad Truitt.

Figure 1.4. Rock core created from rock penetrator.

1.2.2 *Ice Penetrator Laboratory Shots*

The Europa Kinetic Ice Penetrator presented new obstacles that needed to be overcome before large scale testing could begin. Proof of concept for the EKIP landing system, creating an ice plume with an engineered projectile impacting at hyper velocity, needed more rigorous analysis; the channelization of impact ejecta into a plume has not previously been studied. Initial testing with miniaturized penetrator designs was conducted in the RAM Accelerator at the University of Washington Aeronautics and Astronautics Engineering Department. This design compares to the European Space Agency's (ESA) penetrator program, designed to withstand an impact up to 300 m/s (Collinson 2008). The University of Washington penetrator is designed to supersede this impact velocity.

In order to optimize the characteristics of the ejecta, modifications were made to the Asteroid penetrator nozzles. Initially, numerical models of miniaturized penetrator (38 mm diameter) impacts were created. These designs are then shot at high velocities into ice blocks. Impacts velocities reached between 1-2 kilometers per second, with the target blocks varying in size between 35 to 100 gallons of fresh ice. High speed cameras determined velocities, and ejecta characteristics such as plume morphology. Figure 1.5 shows two projectile designs tested. The

"spike" projectile design is most similar to a rocket nose cone or bullet; the hypothesis for this design being a deeper penetration into the ice target. The projectile is made of 6061 Aluminum with a magnetic strip attached to record velocity during testing. The second design, the cylinder projectile, is also made of 6061 Aluminum. Unlike the spike projectile, the cylinder projectile is hollow, with an interior bevel to create a more efficient cutting edge upon impact. The cylinder projectile design is both lighter and was determined to create a more channelized ejecta plume than the spike projectile, though penetration depth was less. (Robinson 2017). The plume created by the cylindrical projectile travels roughly 1/3 the velocity of the impactor, an empirical relationship established by laboratory testing (Robinson 2017).

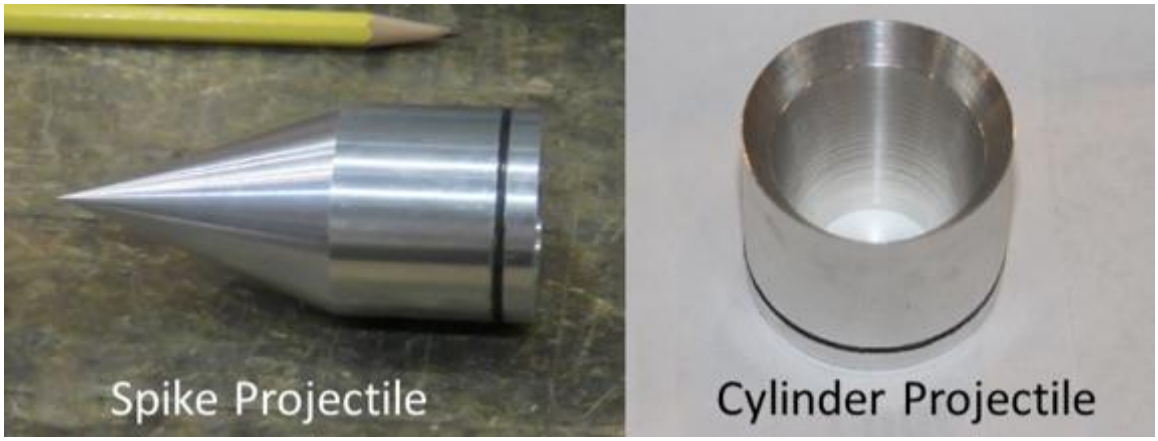

Figure 1.5. Modified ice projectiles. Left: Spike projectile used for initial testing. Right: Cylindrical projectile with interior bevel.

Chapter 2. MICROBIAL IMPACT

Possible microbial life, or an environment able to support microbial life, is a major aspect of the interest in Europa's ocean and ice crust. Ice thicker than a few feet's ability to block radiation (Paranicas et al. 2002) protects any microbial life able to survive in the subsurface ocean from the extreme radiation emitted from Jupiter, as well at the cosmic radiation from the sun.

With the continued interest in possible microbial life in Europa's subsurface, the logistics behind landing on the moon's surface are substantial. Not only must the process of landing be considered, but the effect the landing system has on the surrounding ice must be considered as well. To study possible microbes using the EKIP landing system, it must be ensured the landing technique will not destroy evidence of microbes in the impacted ice. With an initial impact velocity of the penetrator of 4 km/s, it is imperative to determine the effect the impact, shockwaves, and subsequent cratering have on the microbes.

Related research studies have been conducted in regards to the panspermia theory; that extremophilic microbes shielded within an impactor (i.e. meteoroid) not only survive hyper velocity impacts, but spread to the surrounding substrate following impact (Mastrapa et al. 2001). The microbes in Mastrapa et al. are well protected/shielded within the impactor, similar to how shuttles protect astronauts from heat during launch. Instead of protection from heat, the microbes are protected from 'extreme' acceleration and rapid changes in acceleration, which could damage cell membranes. In comparison, this study focused upon microbes contained within a substrate, impacted by an outside projectile. The microbes in our study are much more vulnerable to changes in acceleration, or pressure waves, that could damage cell membranes. The objective of this study is to map where the most damage to the microbes occurs; if the microbe survives, dies, or is completely destroyed within the impact crater.

2.1 EXPERIMENTAL SET-UP

The set-up used for this experiment has been used for numerous previous experiments regarding ice impact shots, utilizing inter-departmental coordination and resources.

2.1.1 *AERB Ram Gun Set-Up*

The Aeronautic Engineering Research Building (AERB) at the University of Washington contains a Ram Accelerator gun, run by Dr. Carl Knowlen. The ram gun is capable of accelerating a projectile more than 8 km/s (Hertzberg, 1988), utilizing similar combustion techniques to that of a jet-engine. In the experiments described below, the gun was used in the "light gas gun mode" where only helium was used and no combustible were present to avoid heating of the ice by any exhaust gases. Some contamination of the ice does occur from by-products that have coated the gun barrel surface from previous combustion experiments.

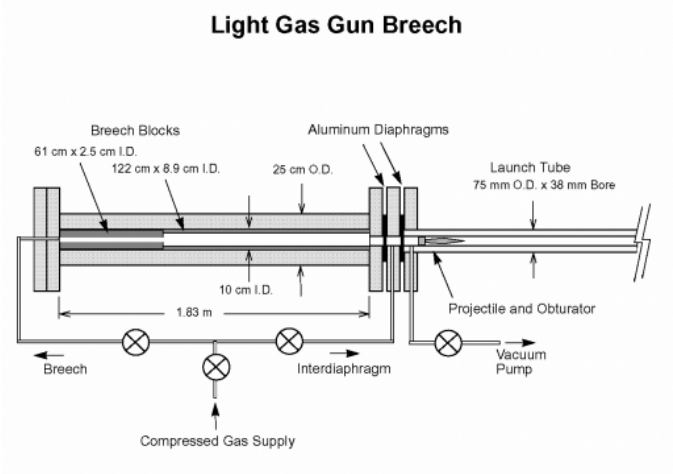

Figure 2.1. Ram gun diagram courtesy of www.aa.washington.edu/research/ramaccel/facility.

For this experiment, the full length of the 40-meter-long barrel was evacuated to near vacuum pressure. The entry diaphragm is made out of 2mm thick plastic film, known to rupture

at pressures able to accelerate the projectile up to 2 km/s. The ice block was held horizontally, a half meter from the exit diaphragm; care was taken to ensure centering of the ice block with the end of the barrel.

Figure 2.2. Ram gun set-up.

2.1.2 *Microbe- Planococcus halocryophilus OR$_1$*

Microbe choice was key for this experiment. The conditions on Europa are more extreme than any on Earth; temperatures ranging from -187.15C to -141.15C on the surface, no atmosphere, and saline waters (Spencer, 1988). An extremophile is an organism evolved to survive in extreme

environments, such as the extreme heat of hydrothermal vents, or extreme cold beneath a polar ice sheet. With assistance from the Fishery Sciences department we chose the extremophilic microbe *Planococcus halocryophilus OR$_1$* (PHOR1) for this research.

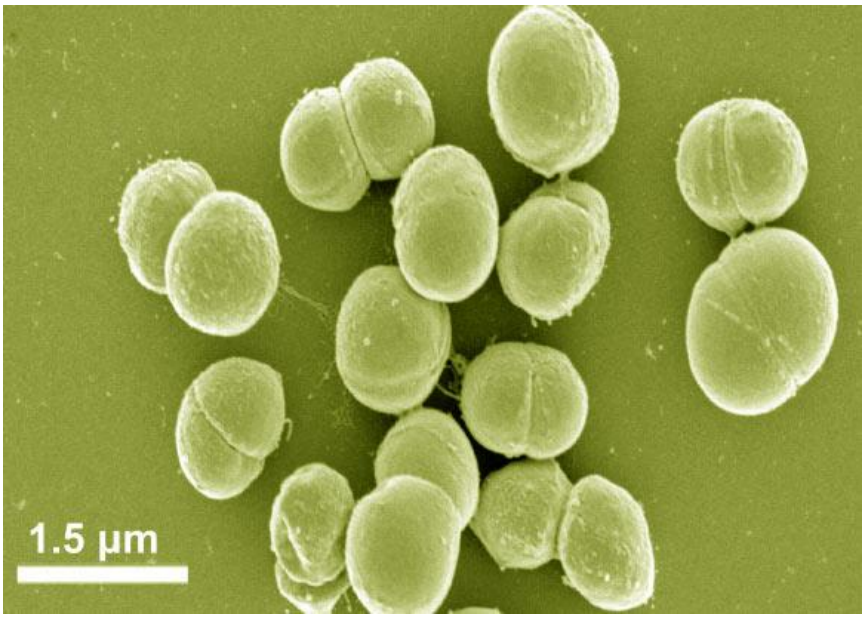

Figure 2.3. Planococcus halocryophilus OR1 (Nadia C S Mykytczuk et al, 2012)

Other extremophiles are able to live in either extremely acidic, basic, anoxic, or irradiated environments. PHOR1 is an extremophile suited to saline, freezing conditions, therefore uniquely suited for this experiment. The microbe is able to reproduce at -16C and survive down to -20C, while being able to hibernate if frozen to -60C with minimal die off (Mykytczuk, 2013). PHOR1 is highly researched previously, and is known as an extremely robust and reliable, easily recognizable microbe to work with. Importantly, PHOR1 has previously been tested with LIVE/DEAD staining, the process planned to determine survivability in this experiment.

Though it is obvious that this specific microbe would not survive the conditions on Europa, it is assumed that if an extremophile is able to evolve to survive the extreme conditions

on Earth, theoretically an extremophile on Europa would be able to match and survive in Europa's environments as well. For this experiment it is not imperative for all the microbes to survive only that some survive the impact. The objective is to prove the impact does not destroy all evidence of life.

The microbes, grown by the Fisheries department at the University of Washington, were grown in a protein solution to provide the microbes with food to reduce die off, and then diluted into two gallons of water. The two-gallon solution was then frozen to -20C over a couple of hours. Though flash freezing with liquid nitrogen would have reduced die off, the process to flash freeze two gallons was impractical for the experiment. The microbes were frozen for less than 24 hours prior to the experiment being conducted.

2.1.3 *Ice Preparation*

The ice used in the experiment was frozen in the Quaternary Research Center's (QRC) D freezer, the same used in the freezing of ice targets for the original EKIP ice test shots. The freezer fluctuates between -35C to -20C through daily defrost cycles. During the defrost cycles, the ice stays cold enough to not actually melt; the purpose of the defrost cycle being to remove any ice on the condenser in the freezer.

The ice block was frozen into a 100-gallon water barrel a meter in diameter. The ice was frozen in layers roughly 10 cm thick, roughly 20 gallons of fresh water at a time. Water chilled to the point of slush forming in buckets was poured into the main barrel to limit crystalline orientation occurring as much as possible. Fresh water was frozen until 30cm from the top of the bucket; 35ppm saline water with a composition of half table salt (NaCl) and half Epsom salt ($MgSO_4$) made up the upper half of the ice bucket. The saline ice formed into a ring with a 30cm high, 30cm diameter cylinder in the middle. That cylinder was then filled with a separately

frozen sample of microbe filled ice. The entire ice block was then frozen for roughly 20 hours before the experiment took place.

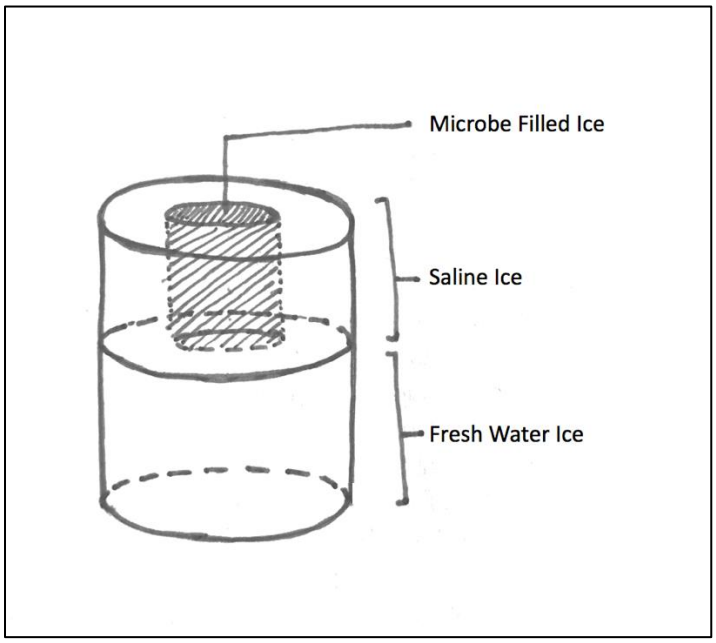

Figure 2.4. Ice block diagram for bio-shot.

Though ice layers may cause boundary effects during the impact (i.e. shock wave reflection over layer boundaries), the freezing process of a singular mass of ice of this size (roughly 800lbs of ice) would be impractical for time requirements for this experiment. Other boundary effects are possible due to the joint of the microbial ice from the saline ice, causing a weak juncture where the two intersect.

An ejecta shield attached to the exit diaphragm of the Ram gun collected samples. This ejecta shield was sterilized using isopropyl alcohol immediately before the experiment took place. Larger debris from the crater collected into a half-meter wide splash bucket, also sterilized using isopropyl alcohol before testing. Factory sterilized 3cm sample tubes collected samples from inside the crater. All samples were stored immediately in a cooler to reduce melting.

The dye LIVE/DEAD from thermofisher stained the microbes to determine survivability. This dye stains living cells fluorescent green, while dead cells and cell remnants stain fluorescent red. This process has the benefit of allowing dead, but not destroyed cells to still be distinguishable, versus stains that only allow visualization of living cells. With help from the Astrobiology lab within the Earth and Space Sciences department, microscopic analysis of a non-frozen control sample, frozen/un-impacted sample, and impacted sample occurred.

As a precaution, DAPI testing was also conducted on both a control and impacted sample of the microbe by the Oceanography and Fisheries departments on campus. This was to ensure a lab bias wasn't an issue, as well as to avoid a staining bias by the microbe. DAPI testing is a more robust stain in regards to longevity of sample life, however the stain only bonds to non-damaged cells, meaning the test would only be beneficial if microbes survived the impact.

Though steps were taken to reduce contamination, the nature of the testing site adds an inherent possibility contamination from the lab, or even the barrel of the gun. Though contamination was a mild concern in this experiment, the chosen microbe, PHOR1, is highly recognizable under microscope. The microbe also cannot survive in fresh water, which means contamination of PHOR1 in the fresh ice sample or water frozen to make the target isn't plausible. As long as PHOR1 is found in impacted samples, contamination by other microbes is less of an issue.

2.2 Results

The experiment was conducted November 2016 in the of the AERB. A 60-gram cylindrical, aluminum projectile was used to impact the ice at 2.2 km/second. High speed camera and GoPro

footage was taken of the experiment. Roughly 29 gallons (0.11 cubic meters) of ice was ejected or removed from the 100-gallon ice block.

2.2.1 *Microbial Survivability*

After both LIVE/DEAD and DAPI staining, it was determined that the microbe Planococcus halocryophilus OR_1 survived the 2.2 km/second impact.

Using LIVE/DEAD Baclite staining, it is visible that small microbes resembling PHOR1 survived the impact, though large amounts of damage and die off occurred. Minor contamination also is visible in both the control and impacted samples. Due to the survival of the planted microbe, the occurrence of contamination is of little concern for this experiment.

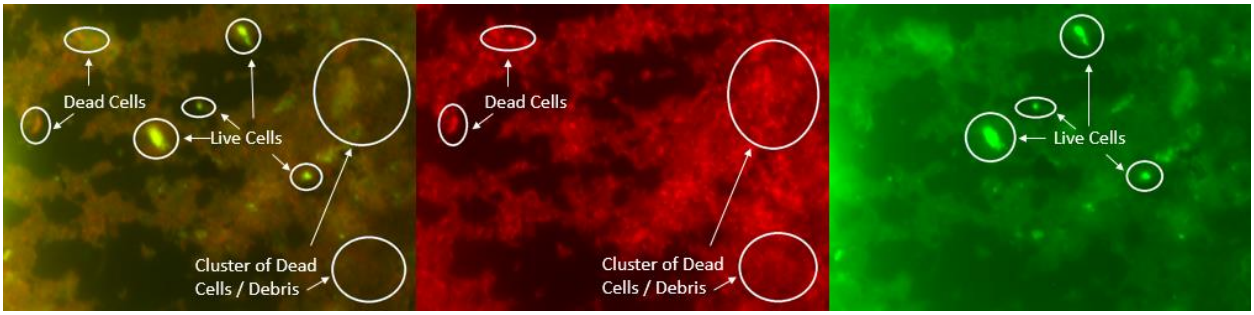

Figure 2.5. LIVE/DEAD staining of the frozen control sample.

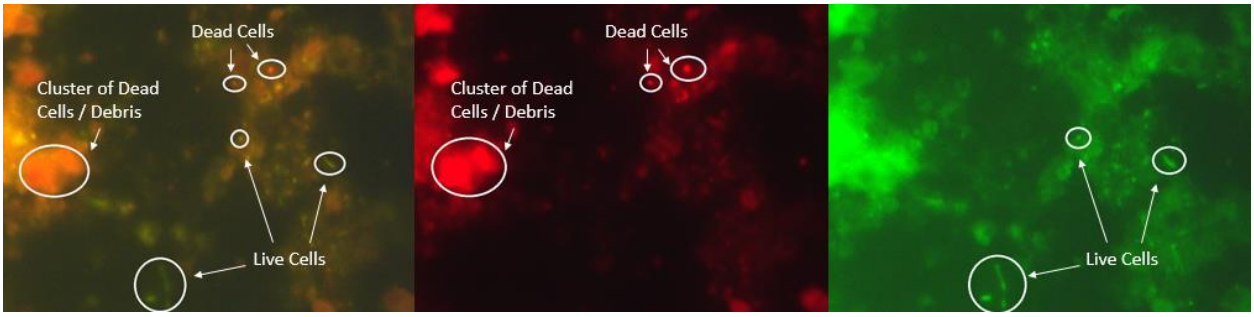

Figure 2.6. LIVE/DEAD staining of the impacted sample.

DAPI staining conducted by the Oceanography and Fisheries department showed similar die off, but confirmed the existence of living PHOR1 cells within the samples from both within the crater and the ejecta caught in the ejecta shield. Similar, minimal amounts of contamination (assumed to be a strain of E. coli) was also noted using the DAPI staining.

Table 2.1. DAPI Staining Results

	RT	8°C	Microscopic observations	Interpretations
C	–	+	**RT:** Few, tiny cells. No growth apparent. **8°C:** Abundance of cells. Single morphology. Resembles 34H.	Evidence for viable 34H cells in samples from SHOT.
E	–	+	**RT:** Few, tiny cells. No growth apparent. **8°C:** Abundance of cells. Single morphology. Resembles 34H.	Evidence for viable 34H cells in samples from SHOT.

Key: 'C' refers to the control sample collected prior to testing. 'E' refers to ejecta collected after testing. 'RT' refers to temperature, as in room temperature. No growth apparent implies the microbe is dormant or inactive.

2.3 Future Microbial Work

The notable result from the experiment is the microbe survived the impact. The lack of complete destruction of the cellular material, let alone the survival of Planococcus halocryophilus OR_1 from a 2.2 km/second impact means the Europa Kinetic Ice Penetrator's impact landing system may be a viable option for the possible research of microbial life on Europa.

Further testing, including more robust freezing must be completed. A fully saline ice block, with higher densities of microbial ice, frozen to higher hardness would remove some boundary

effects from the experiment. Removing layering to an extent would also be optimal. Higher care will also be taken to reduce contamination in further testing.

Beside changes in freezing techniques, the velocity of impacts will be gradually increased in further testing. Increasing velocities up to the predicted 4 km/second impact velocity of the EKIP lander will be necessary to fully rule out possible microbial destruction from the proposed impact landing system. During these tests, characterization of zones within the crater will be analyzed to determine which zones contain the most microbial damage.

Chapter 3. EKIP FIELD TESTING

The initial work on the Europa Kinetic Ice Penetrator impact landing system design has focused heavily on miniaturized versions of the first stage impactor, the penetrator, for laboratory tests. Testing of the full system, including separation of the second stage/payload section as well as electronic survivability, needed to be conducted as part of my research.

Previous, miniaturized designs of the Europa Kinetic Ice Penetrator's impactor system have been tested in the laboratory. These tests, though at high velocities similar to those expected for the mission, boundary effects caused by size restrictions cause issues with crater morphology and shock wave propagation through the ice. Field testing on Easton Glacier of Mt. Baker, WA was planned, but later canceled due to the target area being determined too small of an area for safe operation. A field test was then planned for Juneau, Alaska, to ensure a large enough target area. Existing designs were modified into true-to-scale projectiles to impact a glacier, increasing the boundary limits to effectively infinite proportions (i.e. depth, horizontal path).

The second stage of the EKIP mission, the payload section, needs to have a compact design that can fit with the space restrictions of the spacecraft and at the same time have a large cross-sectional area to attain a sufficiently large braking surface to allow efficient deceleration of the payload section within the generated transient atmosphere. These requirements lead to the conclusion that the payload section must have a deployable surface. Different designs were considered. It was concluded that a shuttlecock design provides the greatest aerodynamic stability and structural integrity for the proposed operating conditions. With this being the initial design, testing of separation, balance, structural integrity, sizing, and material strength must be tested for further designs. Further discussion of the second stage is included in Chapter 4.

This field test, though intended to be a proof of concept for the EKIP landing system, is also being used as the first of several empirical tests to catalogue the morphology of the EKIP lander in ices of differing hardness, such as snow, sea ice, blue glacial ice, and basalt. When the depth and shape of the crater in each hardness substrate is combined into an empirical curve, the results of an impact on an actual icy planetary body can be fit into the curve. This data will give insight into the ice dynamics of the impacted surface in a way remote sensing is unable to. Furthermore, these tests will be used to ground truth the biology laboratory experiments, to ensure the compressional effects seen in the miniaturized shots are still accounted for in true to scale tests.

3.1 Penetrator Design

The first stage of the EKIP landing system, the penetrator, determines the ability of the second stage to slow down. Through the creation and channelization of ejecta from the impact of the penetrator, an artificial atmosphere can be created on Europa, enabling the use of a chute-centric deceleration technique.

The channelized ejecta, or the ejecta plume, must be both dense and fast enough to impart a considerable amount of momentum to the second stage. To ensure this, miniaturized impactors were shot into ice at high velocities. The basic shape of the penetrator was determined, but due to mass and size constraints, the actual design of the penetrator needed to be further designed at larger scale in field testing.

An overview of each of the six penetrators designed for field testing are contained in the table below. For in depth descriptions of each penetrator, see following sections.

Table 3.2. Penetrator Attribute Table

Penetrator	Design	Mass (kg)	Material	Length (cm)	Bore Diameter (cm)
Stumpy	Nozzle	12	A2 tool steel	35	15 max, 7.6 min
Slim Jim	Straight Bore	7.3	Steel, Aluminum	51	7.6
Long John	Straight Bore	9.9	Steel, Aluminum	39	10.1
Firefly	Straight Bore	3.4	Aluminum	22	7.6
Inner Steel	Finless	6.4	Steel, Aluminum	38	10.1
Outer Steel	Finless	4.1	Steel, Aluminum	33	7.6

Figure 3.1. Photo of the four finned penetrators. From the left: Stumpy, Long John, Firefly, and Slim Jim.

3.1.1 *Nozzle Design*

The “nozzle” design of the penetrator mimics that of an actual rocket nozzle. Because the ejecta needs to be kept at high velocity, the design of a nozzle is ideal. Rocket nozzles, using a converging-diverging nozzle design, are able to accelerate propellant, converting thermal energy to directed motion. Utilizing the converging-diverging nozzle, a penetrator should be able to accelerate the ejecta created from impact in a similar fashion. During laboratory testing, the ejecta was accelerated to roughly 1/3 the velocity of the impactor (Robinson 2016). However, during field testing an inert penetrator, the terminal velocity is subsonic, meaning the nozzle cannot accelerate the ejecta. However, this design will be used in future supersonic impacts, so the nozzle design must also be used during the first field test.

For field testing several different designs were considered. The penetrator nicknamed “Stumpy” was designed with the intent to mimic a nozzle. The intent of this penetrator was to maximize mass while minimizing impact surface. A2 tool steel was chosen for its high density to increase mass, as well as its resistance to fracturing. Because the penetrator would only be used for a single impact, the durability was of less importance than maximizing the mass. However, the penetrator had to withstand the impact without significant deformation or run the risk of blocking ejecta flow from misshaping. With a total mass of 11.8 kg, 20 cm length, and 15 cm width, Stumpy is the second smallest, but most massive of the penetrators. The exterior beveled edge, used as a cutting edge, coincides with a straight cut converging angle, into a 7.6cm diameter straight bore. The nozzle then continues to a 10cm long straight diverging cut, extending out to 14.5 cm diameter at the outlet of the penetrator. Four steel fins were welded to the exterior of the penetrator to ensure stable flight. Even with the attached fins, the minimal distance between the center of pressure (CP) to the center of mass (CM) increased the chances

for unstable flight, or tumbling. For this reason, the fins were extended back past the end of the penetrator to extend the distance between the CP and CM.

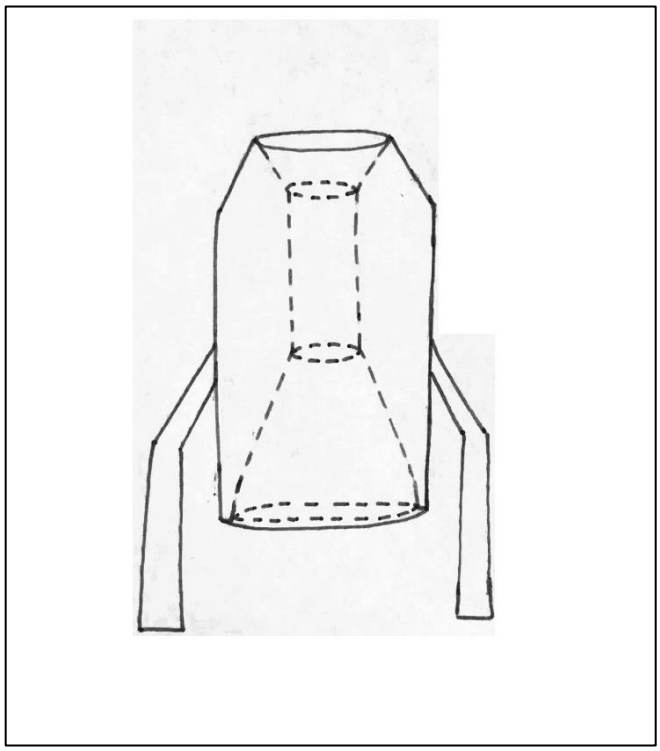

Figure 3.2. Basic schematic of Stumpy. Though not to scale, the interior "nozzle" design is visible.

3.1.2 *Straight Bore*

The second design type, the straight bore, is similar to designs for the nosecone of the asteroid penetrator. As implied, the bore hole of the penetrator in this design is straight, unlike that of the nozzle design. In this design, the leading edge often has an exterior or interior/exterior bevel to create a 'cutting edge' for initial impact. In comparison to the nozzle design, the straight bore design intends for the ejecta to eject en masse, instead of breaking apart and possibly decelerating within the penetrator.

The first straight bore design, nicknamed “Slim Jim” is a dual material design between steel and aluminum. The steel at the leading edge is beveled to decrease impact surface, with a joint continuing into the aluminum. The steel impacting edge has durability and mass, while the aluminum addition increases the over al length. With a diameter of 7.6 cm and length of 51 cm, this design was to maximize stability while falling. With such a long body, the center of pressure in Slim Jim is much more conducive to stable flight than Stumpy. Small fins were welded to the aluminum body to further increase stability. However, due to the excessively long, straight bore, the chances of flow stagnation before ejecta can exit the penetrator increase heavily, as seen in previous testing with the rock penetrator (Truitt, 2016).

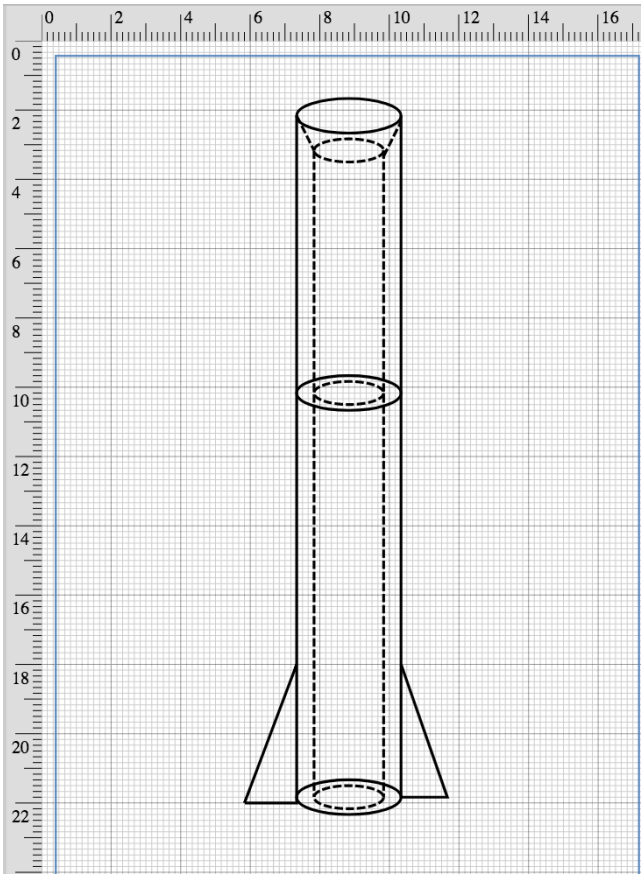

Figure 3.3. Schematic of Slim Jim.

The second straight bore design, nicknames “Long John” is another dual material design of aluminum and steel. With the same material orientation as Slim Jim, as well as the same bevel on the leading steel edge, Long John is extremely similar in design to Slim Jim. However, the name is a misnomer, with Long John actually being shorter than Slim Jim. At 39 cm length and 10.1 cm diameter, this design has a larger impact surface, but is less likely to cause flow stagnation of the ejecta. The wider bore may cause flow deceleration in relation to a smaller diameter bore.

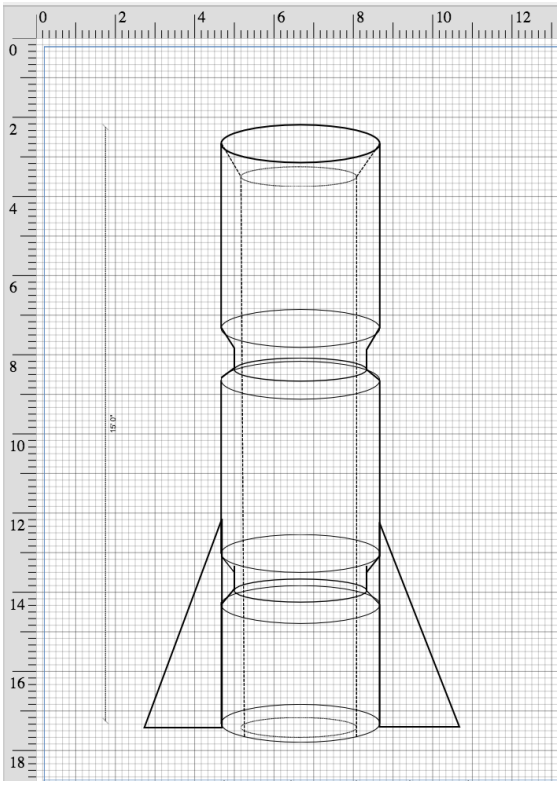

Figure 3.4. Schematic of Long John.

The final straight bore design, with the nickname of “Firefly”, is the smallest designed penetrator. This design is purely made of aluminum, with an interior/exterior bevel on the front edge. Totaling just under 18cm in length and 3kg in mass, Firefly is dwarfed in size by the other designs. With minimal mass, Firefly will have a small terminal velocity in comparison to the

other, more massive penetrators. To increase the mass from the pure aluminum design, iron weights were added to the nose edge of the penetrator. With the minimal length, stagnation of the ejecta is unlikely, though lacking mass and speed may minimize the amount of ejecta created upon impact.

3.1.3 *Finless*

The final penetrator design, the Finless design, was the final to be created. These penetrators were included as a fail-safe for the drop test, created as an attempt to quickly increase the number of penetrators able to be dropped. This was to hopefully increase the probability of a successful test drop, as well as increasing the chances of finding the penetrators after they've impacted. This design is another set of dual material impactors, without a straight bore and without the attachment of fins. This lack of fins reduces air resistance/skin friction during flight, meaning the same mass penetrator has the ability to achieve higher velocities. However, the lack of fins also destabilizes the flight of the penetrator, increasing the chance of tumbling during flight. To reduce tumbling, the penetrators were heavily weighted to the front edge of the penetrators using material weighting.

The first penetrator of this design, Inner Steel, is designed exactly as the name implies. An interior bevel on a 7.6cm diameter steel pipe was cut, with the steel pipe then being inserted into a snuggly fitting aluminum pipe. With the increasing diameter from 7.6 cm to 10.1 cm, a primitive compression zone and divergence was created. With the total length of 38 cm, the primitive nozzle created decreased the chance of flow stagnation of the ejecta. The total mass of the penetrator, 6.4 kg, makes this penetrator the median mass of the penetrators. As mentioned above, the lack of fins on this design may lead to tumbling. To minimize this effect, the penetrator was heavily weighted with towards the leading edge. This was done using the conjoining of steel and aluminum. With a

large ratio of steel to aluminum, the majority of the mass lies in the leading end. However, due to the steel portion being extremely long, the mass is spread up into the penetrator instead of being focused near the leading edge. This could cause an additional lack of stability.

The second finless design, Outer Steel, is yet again designed as the name implies. Going from a beveled 12.7 cm bore steel tube to a 10.6 cm aluminum tube, all ejecta entering the penetrator is compressed. This primitive nozzle design may cause an increase in ejecta velocity, though at the minimal extent could lessen flow stagnation in the ejecta flow. With a total length of 33 cm, and the steel extending only 10 cm, the majority of the mass is weighted at the leading edge of the penetrator. This weighting of the material will hopefully counteract the destabilization caused by the lack of fins. Outer Steel, being 4.1 kg, is the 2nd smallest penetrator designed.

3.2 PENETRATOR DROP

Field testing for the Europa Kinetic Ice Penetrator's drop test was conducted from 17 July 2017 to 23 July 2017 on the Juneau Icefield, Alaska. The actual drop test occurred on 20 July 2017 on the Taku Glacier, through coordination with the Juneau Ice Research Program.

Figure 3.5. The Taku Glacier with the Taku Towers in the distance. The drop site is directly below the Towers onto the center of the glacier. The hole pictured is the mass balance hole shown in Figure 3.7.

Figure 3.6. Camp 10, the base of operations for the drop test, operated by the Juneau Ice Research Program.

The Taku Glacier, a 386mi^2 Alaskan tidewater glacier, sits at an elevation of 4700 feet above sea level at the site of the drop. The glacier was covered in an annual snow layer roughly 2m thick. The annual snow had an average density of 0.42g/cm^3, interspersed with two to three ice lenses, indicated on the figure below. The local geology consists of feldspathic granite interspersed with quartzite dikes. Cobbles from a nearby nunatak were collected for additional drop test projectiles. The Taku Towers, granitic peaks standing at 1597 m, were used as the minimum allowable cloud ceiling for the drop to occur. A helicopter provided by Coastal Helicopters was used for the drop.

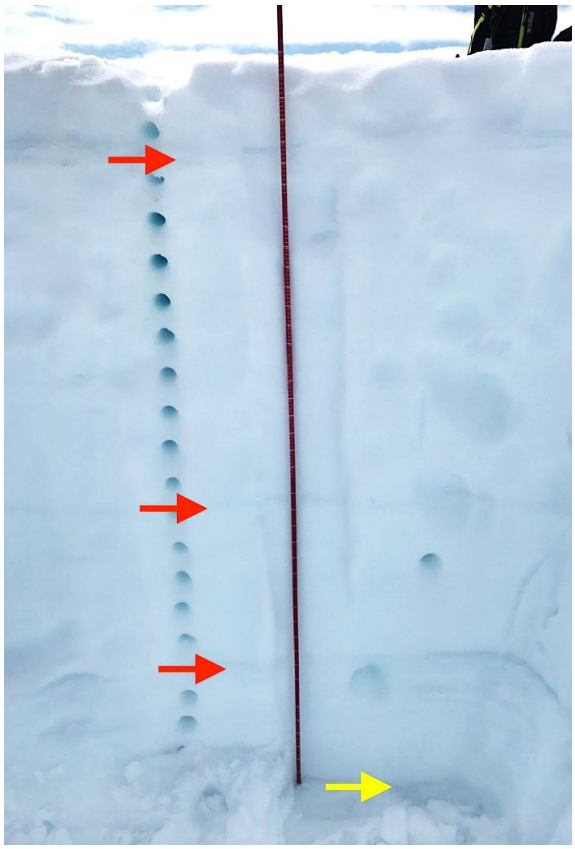

Figure 3.7. Ice balance pit dug out by JIRP. Density measurement holes along left side of image, measurement probe for scale. Ice lenses indicated by red arrows, beginning of firn layer indicated by yellow arrow.

Figure 3.8. The helicopter, piloted by Coastal Helicopters, above Camp 10. Projectiles were slid out of tubes from open door. Three separate flights were needed for all drops to occur.

3.2.1 *Control Impactors*

While the overall goal was to test the specifically designed penetrators and document the differing effects of each design, it was also necessary to compare the craters created by the penetrators with those of natural impactors (i.e. rocks). Though impact cratering is heavily studied, the majority of the studies focus on impacts at high velocities. This test will focus on low velocity impacts. Though a rough comparison, similarities between the rock craters and high velocity impact craters known to impact theory can be shown. With the same comparison, the low velocity impact craters can be extrapolated to predict crater morphology of high velocity penetrator craters. Future high velocity field testing will further compare and hopefully validate this relation.

In order to accurately compare craters from the penetrators, cobble sized rocks of similar masses to the penetrators were dropped. These rocks, chosen from a scree hill on a nunatak, are the same composition as the surrounding geology. Through classic impact theory, the crater's typically have depth to diameter ratios between 1:5 and 1:7 (Osinski, 2013), regardless of speed or size of impactor. This characteristic ratio creates a shallow, wide crater with specific ejecta patterns, shown in the figure below. The craters created during the field test lack several key components from Osinski's diagram, shown below. The ejecta ad allochthonous crater-fill deposits are not present due to the low impact velocity. The impactor in hypervelocity impacts is usually destroyed, while the rocks dropped were notably still present. The broken up substrate shown with the rock craters could be analogous to the impact breccias referred to in the figure. The rock craters fall under the category of "simple craters", which are roughly bowl shaped and are controlled through compressional forcing. Because of the low velocity impact and the effect of gravity, the rock craters create more of a pit than a traditional crater shape.

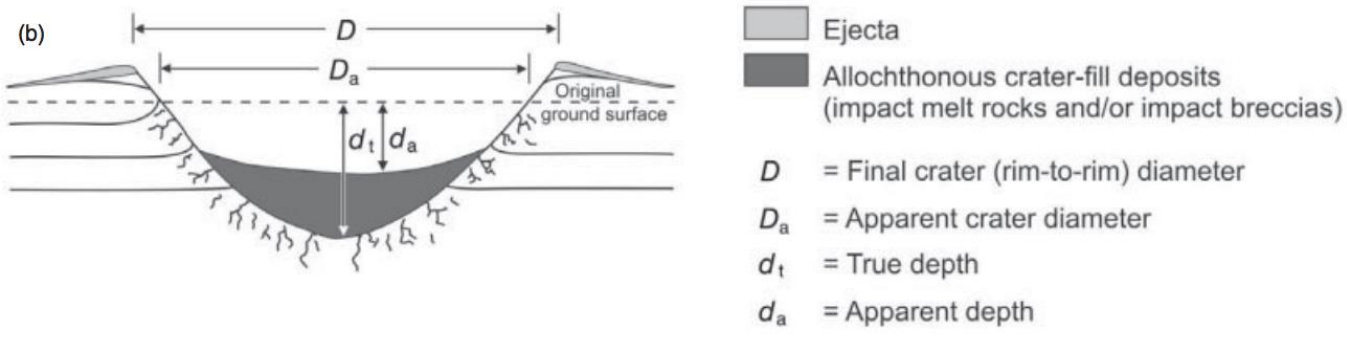

Figure 3.9. Typical crater morphology of an impact crater. Similar to what is expected from the control rocks dropped during the test. Figure modified from Osinski, 2013

The control rocks were 7.26kg, 9.98kg, and 11.34kg, chosen for their roughly spherical shape in order to imitate natural impactors. Though impactors this size (i.e. meteoroids) would burn up in Earth's atmosphere, the lack of atmosphere on Europa would enable smaller impactors to reach the surface. The rock crater created by the 11.34kg rock, measured to an apparent depth of 0.5m, a true depth of 1.1m, and a diameter of 1m. Thus, the rock crater's depth to diameter ratio stands at 1:2. Though a smaller ratio than normally seen with natural impactors, this can be explained by the low velocity of the impact.

3.2.2 *Engineered Impactors*

Based upon laboratory experiments, the engineered impactors, the penetrators, have a distinctive crater morphology completely different from that of a natural impactor. When impacted at mid to high velocities into blocks of ice, the penetrators have a typical depth to diameter ratio of 3:1 to 5:1 depending on the velocity of impact. This reversal of the depth versus diameter ratio in comparison to natural impactors is most likely caused by the excavation design of the penetrators. With the large impact surface on natural impactors, the majority of the force of impact is imparted both horizontally and vertically. The momentum separated into the horizontal direction increases the substrate fracturing in the horizontal plane, while reducing the depth of the crater. While ejecta from natural impactors typically reenters the crater or is deposited on the rim of the crater, ejecta from the penetrators is shown to evacuate the crater almost entirely, with side walls of the crater typically caving inwards.

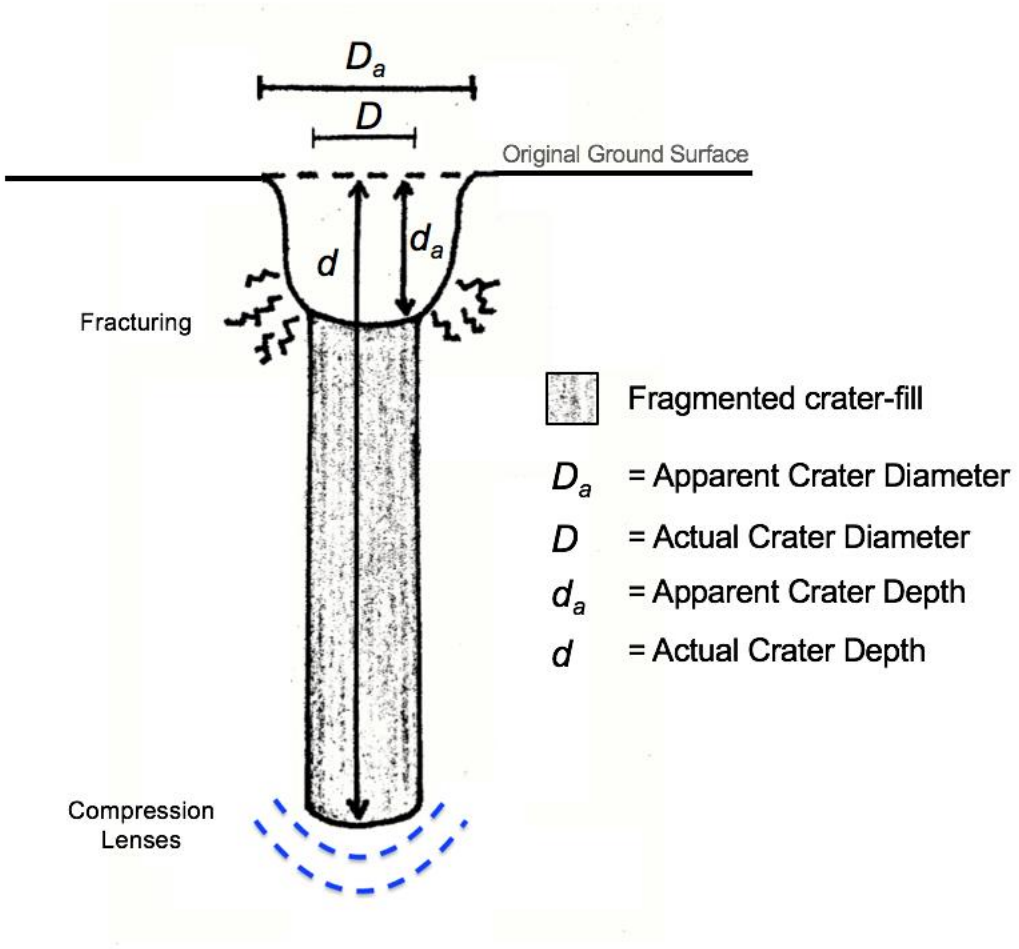

Figure 3.10. Diagram of penetrator crater.

The penetrators also have a distinctive plume of ejecta in the laboratory shots, a characteristic unlikely to occur in the field test due to low velocities and soft, wet snow as a substrate.

3.3 Penetrator Results

Wind conditions for the drop averaged 10knots from the South at the helicopter, 10knot, katabatic winds from the North at ground level. Cloud base was roughly 4000 feet above the glacier; Projectiles were dropped roughly 2500 feet about the glacier. Due to the crossing wind patterns

during the drop, the projectiles scattered along a roughly 1 km cross section of the glacier, shown in the map below.

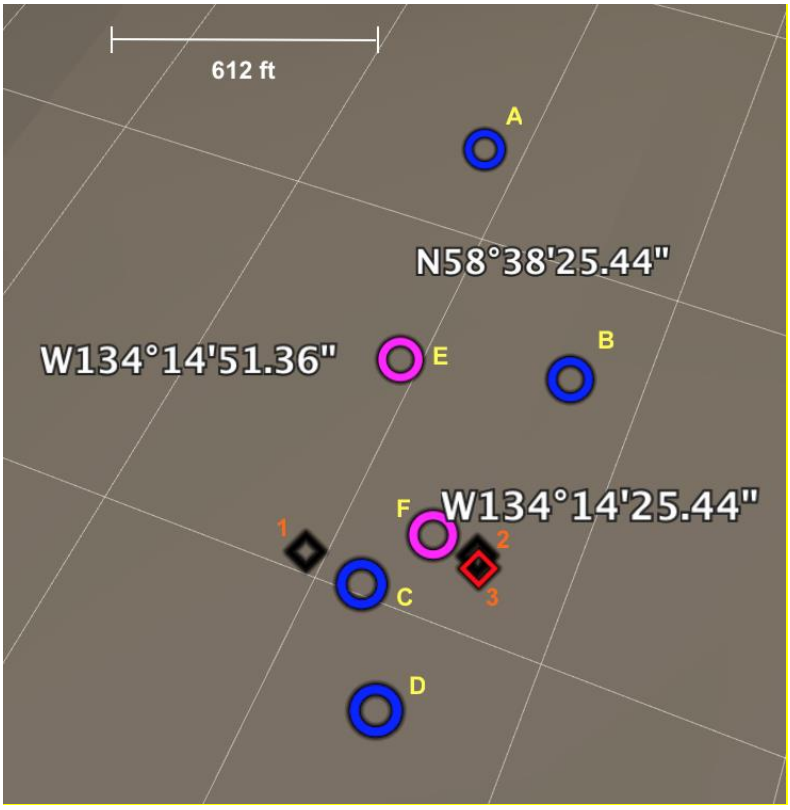

Figure 3.11. Projectile drop map. Key: (Circles)penetrators, (diamonds)rocks. (Blue, Black) Density measurements. (Pink, Red) no density measurements. (A)Slim Jim, (B)Stumpy, (C)Long John, (D)In. Steel, (E)Fire Fly, (F)Outer-Steel. (1,2,3) Rocks.

3.3.1 *Crater Morphology*

The cratering between the cobbles and the penetrators was highly different. The cobbles showed the characteristic impact crater hypothesized thought impact theory: the craters were relatively shallow and wide. However, the rock craters were deeper than typical natural impact craters, possibly due to the extremely soft substrate and low velocities.

The overall shape of the craters created by the penetrators had an average depth to diameter ratio of 19:1 to 20:1. This extreme ratio difference between not only natural impactors, but laboratory shots, could be explained yet again by the low density and highly compactible substrate. Unlike the ice in the laboratory shots which fractured upon impact, the snow in the field test acted more like a cookie cutter going through clay during impact.

Density measurements were taken at multiple crater sites, including a rock and four penetrators. A map of craters with density measurements taken is shown below. Detailed density measurements for each crater can be found in section 3.3.2.

3.3.2 *Individual impactors*

The impactor section will focus on each individual crater created by each penetrator. Craters created by the rocks will be used for comparison purposes only.

Stumpy

The crater created by Stumpy, shown in Figures 3.23 through 3.25, was the second deepest crater created. With a depth, measured to end of penetrator, of 1.84m, and diameter of 0.12m, the crater has a depth to diameter ratio of 15:1. The reversal of the ratio between the penetrator and the rock crater agrees with results from laboratory shots.

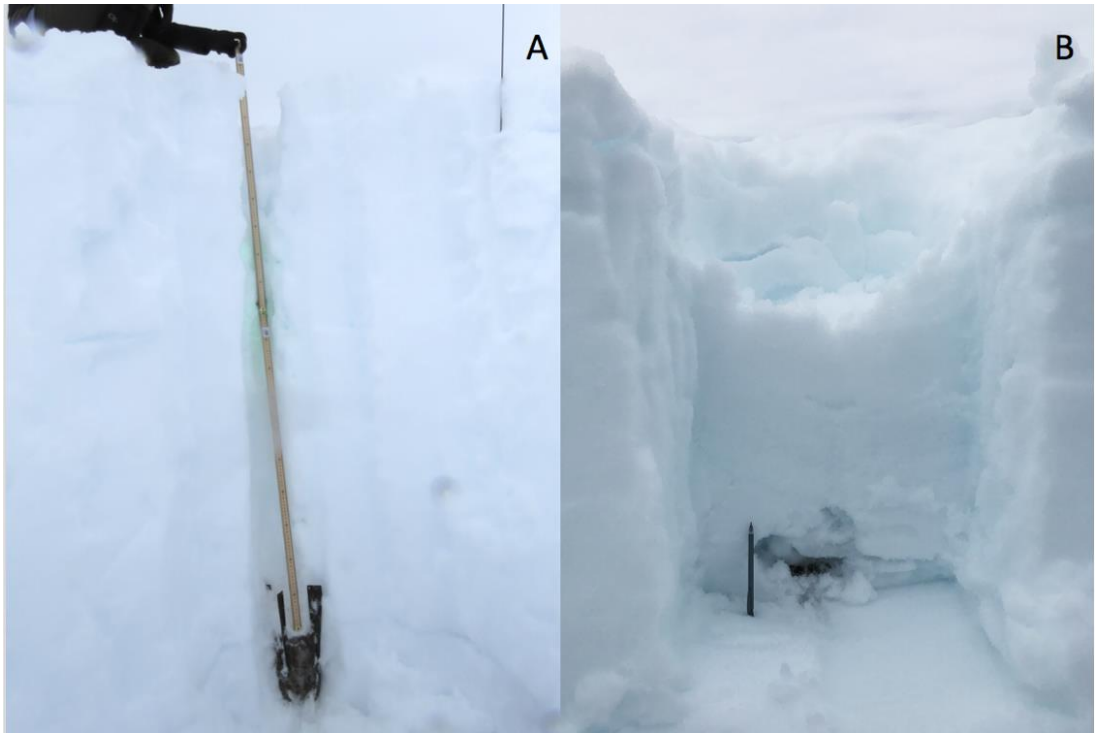

Figure 3.12. A: Full depth of Stumpy's crater, measured to the end of the projectile, measured to 1.84m. This image was taken after crater infill was removed. B: 11.34kg rock crater, apparent depth measured 0.5m, true depth 1.1m.

No plume was created by the impact of this penetrator. However, through examination of the crater, the nozzle design began the process needed to create a plume. The nozzle penetrator is designed to compress and then expand material passing through the nozzle. This process pulverizes material, and though difficult to see in snow, the destruction of ice lenses impacted by the penetrator, as shown in figure 3.13, clearly show that material going through the nozzle is not merely being slid past like a cookie cutter. Further evidence of this process can be seen in the density measurements taken. As shown in figure 3.14, the crater infill leftover from the penetrator passing through the ice shows evidence of being broken up. The density of the surrounding annual snow layer averages 0.45 g/cm^3 throughout this area of the glacier. The crater infill has a density of 0.41 g/cm^3, while the density of the snow directly below the penetrator was measured to be

0.61g/cm^3. These measurements, along with all the density measurements, were taken roughly 48 hours after impact the impact. This means refreezing will equalize densities to a minor extent. This means that the lower density of the infill may have been initially lower directly following impact. Regardless, the lower density infill, and lack of evidence of wall collapse, could mean the pulverized snow/ice in the infill would have been evacuated into a plume had the penetrator impacted at a higher velocity. The higher density snow seen below the penetrator is mostly likely caused by compression waves as the penetrator lost momentum and flow stagnated within it.

Figure 3.13. Close-up of Stumpy before surrounding snow and ice was removed. Visible ice lens outside the penetrator, indicated by finger, is not present inside the debris snow within the penetrator. This indicated the ice lens was pulverized upon impact.

Figure 3.14. Stumpy's crater prior to removal of crater infill. Colored squares indicate where density measurements were taken: Orange – Control 1, Blue – Control 2, Red – Sample 1, Green – Sample 2.

Table 3.3. Crater Density Table – Stumpy

Sample	Control 1	Control 2	Sample 1, Tunnel	Sample 2, nose
Depth, cm	75	75	75	210
Mass, g	43.40	44.90	41.10	60.50
Volume, cm^3	99.00	99.00	99.00	99.00
Density, g/cm^3	0.44	0.45	0.42	0.61

Slim Jim

The long, welded, two material penetrator Slim Jim, was the first penetrator to be excavated. Though the penetrator impacted to a smaller depth than Stumpy if measured to the end of the penetrator, Slim Jim impacted the largest depth when measured to the nose of the penetrator. Slim Jim's nose impacted the firn layer, making this the only penetrator to penetrate all the way through the seasonal snow layer. Blue dye used to mark the impact zone colored the crater infill. This penetrator crater had a depth to diameter ratio of 10:1. The smaller ratio of Slim Jim than Stumpy may be accounted for by the mass difference, and subsequent velocity difference between the two penetrators.

The crater shape from above of Slim Jim versus the rock crater, shown in figure 3.27, differ substantially. The penetrator crater appears as if the penetrator cut straight through the snow upon impact, similar to that of a cookie cutter. Clear impressions of where the fins impacted is visible. A small amount of debris can be seen along one side of the penetrator crater, possibly due to the penetrator impacting at a small angle before straightening. Another possibility could be that the penetrator had a slight spin upon impact, causing debris to be created. However, due to the asymmetric occurrence of the debris, it is most likely that the penetrator came in at a small angle.

The impact created an ice core of compressed layers from the annual snow, shown in figure 3.17. The layering could easily be seen with the naked eye. Upon the accidental drop of the core, the core easily broke apart into individual layers, believed to be snow events of the annual snow compressed into ice. Density measurements of the crater were completed, with crater infill being slightly less dense than the control snow around the crater. A sample taken from below the nose of the penetrator showed a higher density 0.13 g/cm^3 higher than the control. This is believed to be due to the compression caused by the ice core building beneath the penetrator, forcing snow

beneath the penetrator to become denser. Unfortunately, density measurements could not be taken of the ice core.

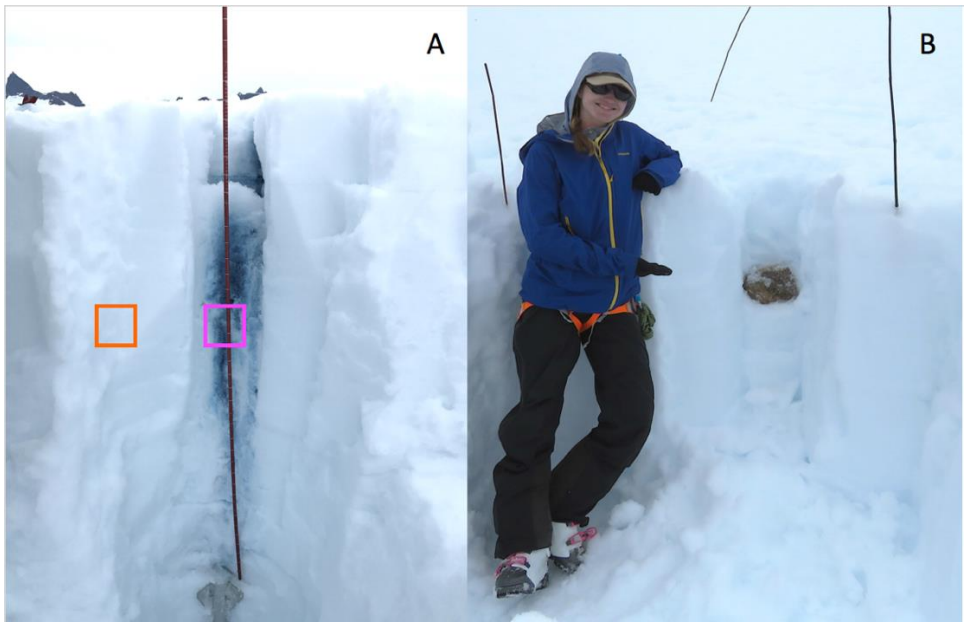

Figure 3.15. A: Full depth of Slim Jim's crater, measured to end of penetrator, 1.5m. Colored squares correspond to density samples: Orange – control, pink – sample 1, sample 2 not shown. B: Corresponding rock impact measured to actual/apparent depth of .3m, width of .4m.

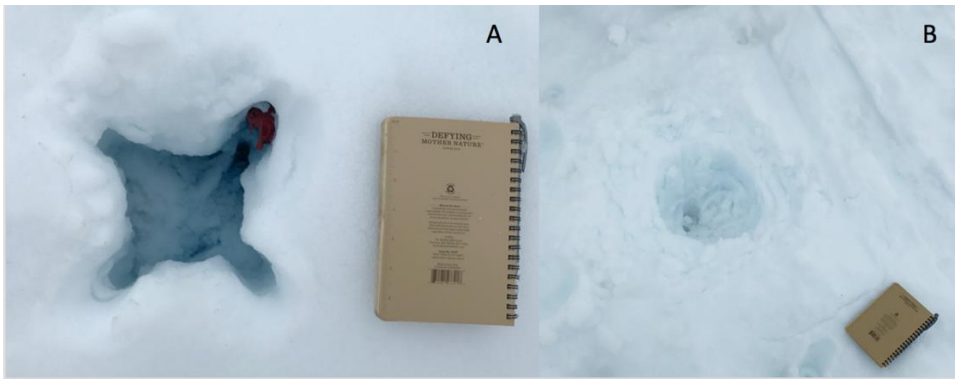

Figure 3.16. A: Top view of Slim Jim's crater. Very little ejecta created, clear marking of where fins impacted. B: Corresponding rock impact crater from above. Wide, shallow crater created, with minor ejecta forming a crater rim.

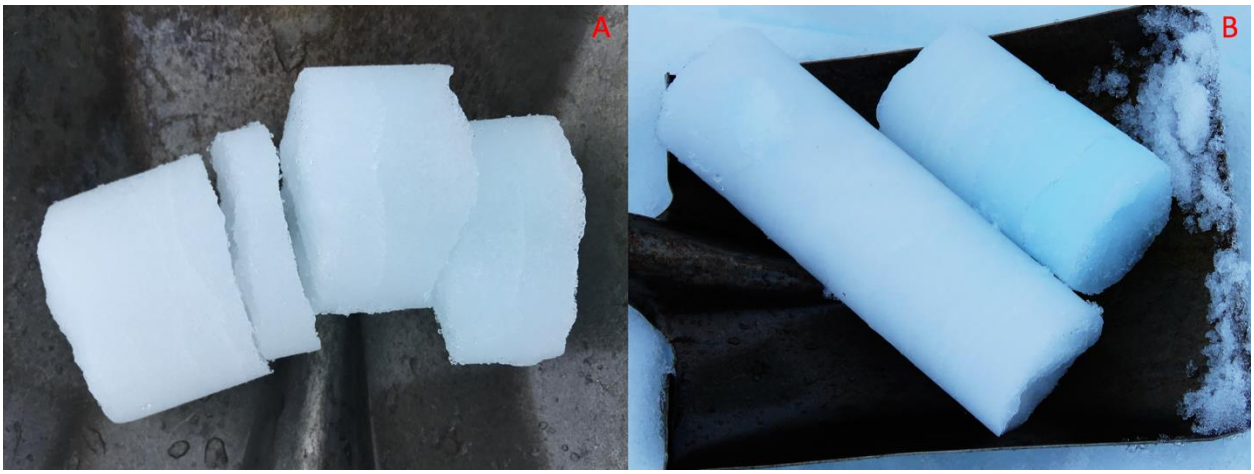

Figure 3.17. A: Core created from Slim Jim impact. Core was removed from penetrator during removal of penetrator from crater. The very front of the core was still attached to the firn layer impacted by the penetrator and was unable to be removed.

Table 3.4. Crater Density Table – Slim Jim

Sample	Control	Sample 1	Sample 2
Depth	30cm	100cm	230cm
Mass	44.50	42.00	57.50
Volume	99.00	99.00	99.00
Density	0.45	0.42	0.58

Long John

The crater created by Long John, shown in Figure 3.18, was excavated the second day. The penetrator impacted to a depth of 1.3m to the end of the penetrator. The crater had an average measured width of 13.9cm, giving the crater a depth to diameter ratio of 9.4:1. Of the penetrators that came in perpendicular, this one penetrated the least. This may be due to the similar mass to Slim Jim, yet larger drag due to surface features. That same surface feature likely caused

compression halfway through the penetrator as the projectile traveled through the snow. As shown in part A of figure 3.19, slight deformation can be seen leading away from the surface indent in Long John's steel portion. In comparison to compression features caused by the rock impact, as shown in part B of figure 3.19, Long John's surface feature caused minimal deformation.

Figure 3.18. Crater created by Long John. Penetrated to a depth of 1.2m at end of penetrator.

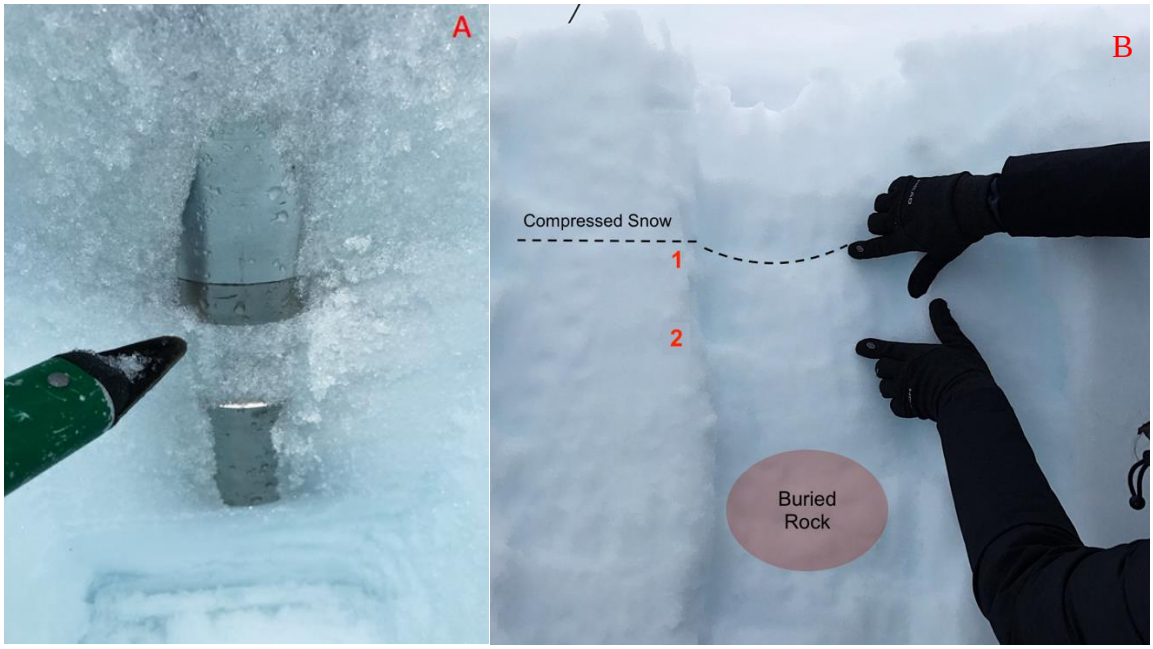

Figure 3.19. A: Possible compression lines created by a surface feature on Long John. B: Compressional lines horizontally parallel to the 9.98kg rock.

As with Slim Jim, Long John also created a snow/ice core. The core, shown in Figure 3.20, corresponded only to the length of the penetrator, unlike Slim Jim's which extended behind the end of the penetrator. This core exhibited no layering, leading to the conclusion that flow did not stagnate until the penetrator stopped moving. In comparison to Slim Jim's core, which showed evidence of flow stagnation halfway through impact, Long John's core shows that the wider bore throat, along with a shorter throat, lessens the chance of flow stagnation. Surface features on the core itself indicate either the snow spiraled while flowing through the penetrator, or more likely the penetrator was still spiraling at depth. The core is noticeably denser than the surrounding snow, including that of the chute. This is most likely due to the compression the snow underwent while flowing, and subsequent refreezing. Based upon malleability testing conducted upon removal, the core created by Long John was noticeably easier to indent than the core created by Slim Jim, indicating the density of the core created by Slim Jim was denser than that of the core created by

Long John. This could mean the snow in Slim Jim's core was much more compressed than that of Long John's, even though the impact velocities should have been similar. This would indicate the larger bore penetrator allowed less stagnation than the smaller bore penetrator.

Figure 3.20. Ice core created by Long John.

Table 3.5. Crater Density Table – Long John

Sample	Control 1	Control 2	Core 1	Core 2	Sample 1, chute	Sample 2, nose
Depth	50cm	50cm	N/A	N/A	50cm	215cm
Mass	49.00	48.00	421.00	354.50	47.50	53.50
Volume	99.00	99.00	628.32	477.52	99.00	99.00
Density	0.49	0.48	0.67	0.74	0.48	0.54

Inner Steel Finless

The Inner Steel finless design penetrator impacted at an angle, curving slightly once it penetrated into the snow. Because of the non-perpendicular impact, the penetrator achieved very little depth. The depth to diameter ratio for this impact is slightly skewed due to the impact angle, with the actual diameter being difficult to determine at the entryway of the crater. Using the

diameter near the end of the penetrator, the depth to diameter ratio stands at roughly 4:1. An interesting feature of this impact is the “nose-bulb” of ice created at the nose of the penetrator, shown in Figure 3.21. This feature was likely created as a result of flow stagnation. The flow most likely stagnated instantly upon impact because of the low impact velocity, as well as the impact angle imparting much of the force downwards while the penetrator went sideways. The remaining force in the penetrator, combined with the larger compressional face, created a larger compressional wave, a bow shock of sorts, at the lead of the penetrator. When the penetrator ceased movement, the compressional wave compressed the surrounding snow into a spherical ice lens. The density of the nose bulb was .2 g/cm^3 higher than the control, and slightly higher density than the core and chute.

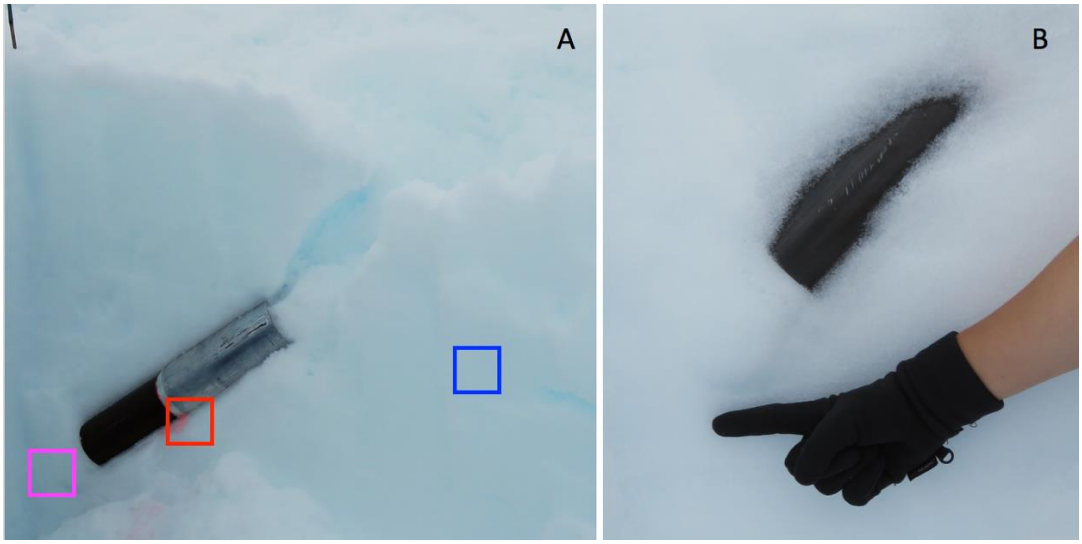

Figure 3.21. Impact crater of Inner Steel finless design. A: Full crater with colored squared indicating density samples: Blue – control, red – steel/aluminum transition, pink – nose bulb. B: Close up of the nose bulb.

The Inner Steel finless design also created a snow core upon impact. It’s doubtful that flow actually occurred with this impact, with the resulting core most likely being the result of a cookie

cutter effect. An interesting effect with the core, as shown in figure 3.22, is the change in diameter corresponding to the expanded inner diameter of the second half of the penetrator. Because the snow had to first go through the smaller diameter opening, the snow had to expand into the second, larger half. This is most likely a pressure effect while refreezing due to the lack of other evidence of flow.

Figure 3.22. Core created by Inner Steel finless design.

Table 3.6. Crater Density Table – Inner Steel Finless

Sample	Control	Core	Nose Bulb	Steel/Al transition
Depth	15 cm	50cm	100cm	75cm
Mass	36.00	37.00	49.60	48.00
Volume	99.00	84.82	99.00	99.00
Density	0.36	0.44	0.50	0.48

Outer Steel Finless

Due to the lack of fins and miss-weighting of the Outer Steel finless design, the penetrator tumbled during deployment and continued in a flat spin throughout flight. This lead to extremely minimal velocity upon impact, as well as the penetrator landing flatly on its side. No true crater was formed by this impact.

Figure 3.23. Out steel finless landing position. Due to a flat spin, the penetrator impacted on its side.

Firefly

The smallest penetrator, Firefly, impacted at very low velocity. The minimal mass of the penetrator led to a depth of only 10cm, resulting in a depth to diameter ratio of roughly 2:1. The penetrator lost a fin during flight or impact and was not retrieved. A second fin broke upon impact, as seen in Figure 3.24.

The impact created a cookie cutter-like snow core. The core was extremely unconsolidated, less so than the surrounding snow. Because of this, it may be possible that the material in the core may have ejected had the penetrator impacted at higher velocity. However, it is also possible that the material would have stagnated and been buried with the penetrator.

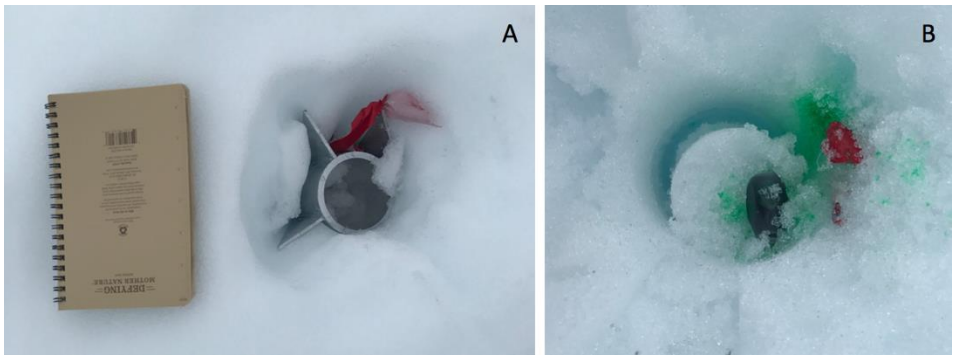

Figure 3.24. Impact of Firefly. A: Depth of crater to end of penetrator only 3cm. B: Crater with penetrator removed.

Figure 3.25. The “core” created by Firefly, more similar to a cookie cutter.

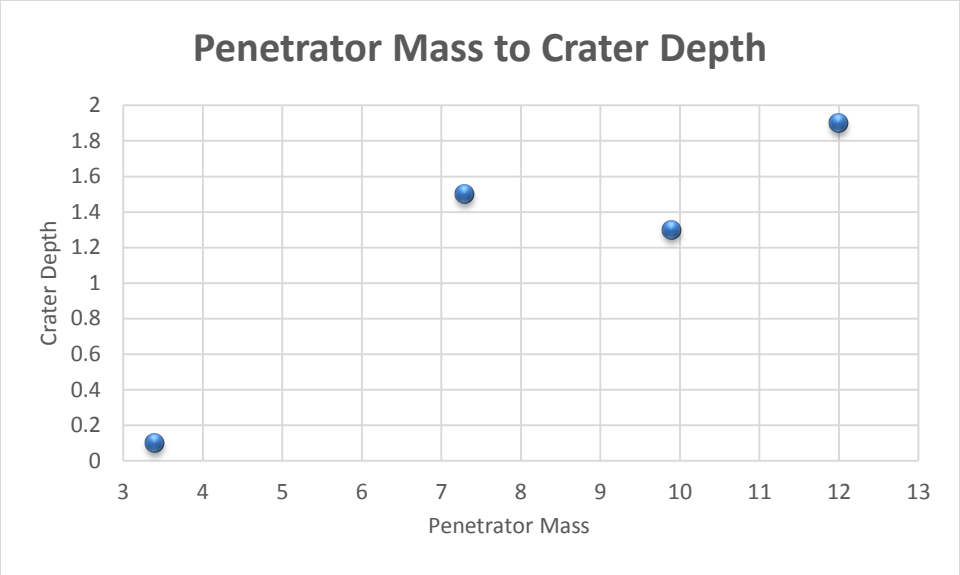

Figure 3.26. Plot of penetrator mass to crater depth for the finned penetrators. The more massive penetrators impacted deeper. However, a definitive relationship cannot be implied due to multiple untracked variables.

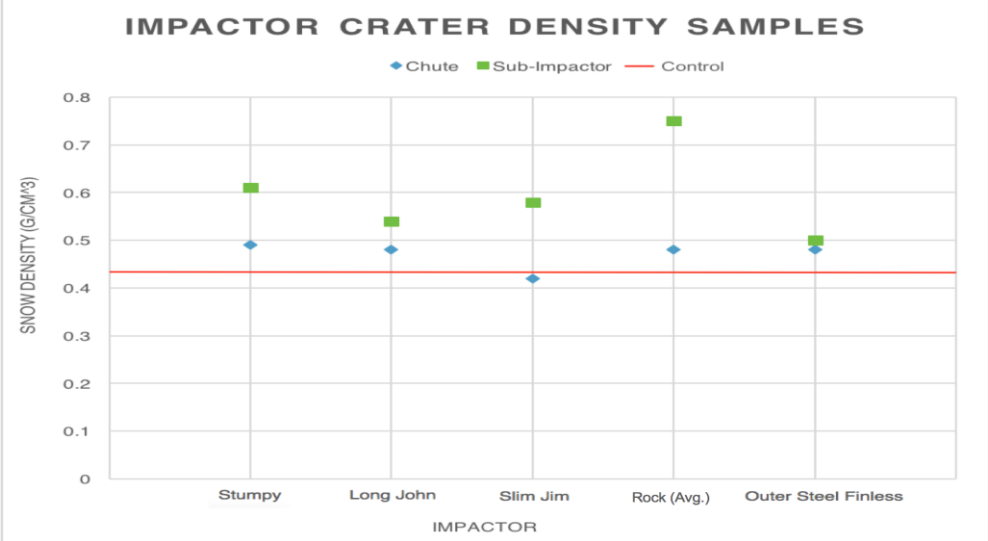

Figure 3.27. Plot of impactor to snow density. ‘Chute’ refers to the path the penetrator/rock traveled through the snow. The sub-impactor density for the rocks was much higher than that of the penetrators.

3.3.3 *Field Test Results and Summary*

The field test of the EKIP system had multiple objectives, with focus on both science and engineering goals. The engineering goal, to test the effectiveness of different penetrator designs, was not truly completed with this field test. Due to low velocity impacts, as well as the low hardness of the substrate impacted, a plume was not created. Future field tests at high velocities will be needed to fully test this component.

The science objective, to use crater morphology of penetrator craters to create an empirical curve, was moderately successful. With a low hardness, the impact into snow will be the lower end member on a hardness constraining curve. However, a high velocity impact into snow would yield more accurate data for future studies. The characteristic morphology of the penetrator craters into snow, together with further data points into harder substrates with future field tests will allow a reasonably accurate extrapolation to apply to an actual impact on Europa.

Chapter 4. SECOND STAGE

The EKIP mission's goal is to successfully land a scientific payload onto the surface of Europa: That scientific payload necessitates the engineering of a second stage robust enough in design to survive the descent through the plume and the impact while protecting the instruments inside. The electronics payload is yet to be determined, but may include motion sense microscopes, seismometers, or magnetometers.

Due to the mass restrictions accorded to space travel, the second stage must be both robust in strength and light in mass. The second stage must withstand high velocity debris as it interacts with the plume. This field test was intended to determine whether the chosen design, which was compact and light, was able to deploy from the first stage, and to determine if the flight was stable. Future testing would be necessary to refine designs to increase mechanical strength.

4.1 Second Stage Design

4.1.1 *Birdie Design*

The penetrator is projected to impact the surface at roughly 4 km/s (Winglee 2018), with the second stage hopefully slowing to 1km/s upon impact. To achieve a momentum-transfer of 3 km/s or more from the ejecta to the second stage, a large surface area is needed to interact with the ejecta. The entire second stage needs to remain as light as possible to decrease the momentum needed to slow it down. The combination of these two requirements, a large surface area with minimized mass, led to two competing designs for the second stage.

The first design resembled an umbrella attached to the end of a rocket. The arms, made of aluminum, were extremely robust, however the arms were minimal in length to conserve an already considerable mass, measuring 1.3ft^2 in surface area. To balance the mass contained at the rear of the lander, the nose of the lander was weighted with lead. The overall mass of the lander, sans electronic payload, weighed 17lbs. The large mass, combined with the minimal surface area caused concern.

The second and working design was adapted to mimic the flight dynamics of a badminton shuttlecock, or birdies. This design allows for a large, lightweight, and stable lander. Due to the shape of the "fins", the birdie requires little to no mass to fly stably. After construction, the average birdie weighed 2lbs, with a surface area of 18ft^2. Springs connecting the two metal bulkheads exert a constant pull to open the birdie. To stow the birdie, the springs must be fully stretched, which may fatigue the springs over long duration stowage.

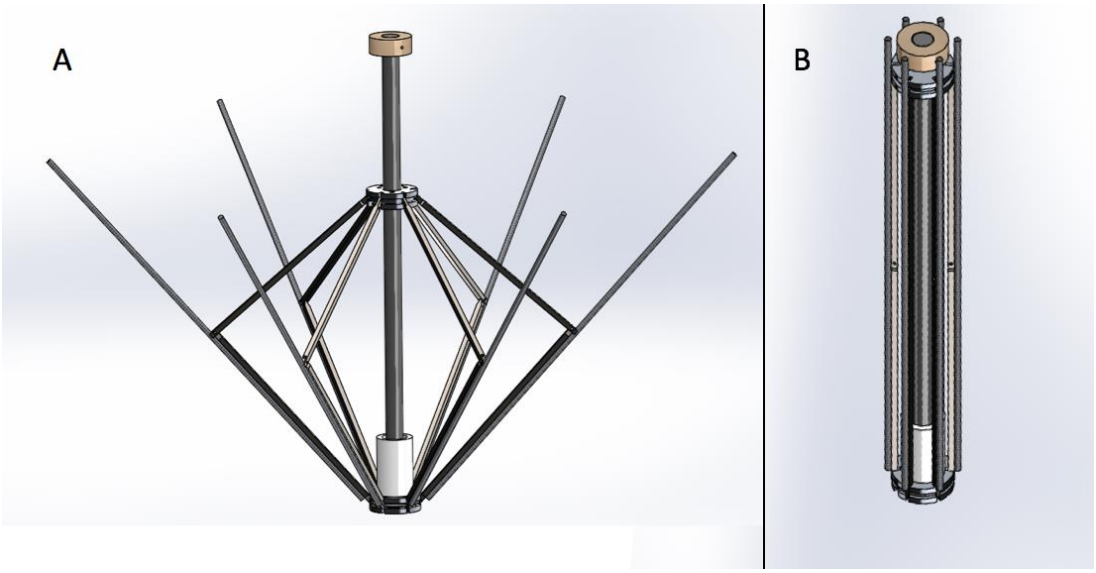

Figure 4.1. Birdie design without chute fabric. A: Design mid-way open. B: Arms stowed.

Figure 4.2. Birdie design with chute fabric. Penetrator shown attached to front, electronics to the top. A: Design mid-way open. B: Arms stowed.

4.1.2 *Construction*

To reduce mass while ensuring the survivability of the lander, material selection was put under much consideration. For an actual lander meant to land on an icy moon such as Europa, the skeleton would need to be a strong, lightweight metal such as titanium. The chute for the actual lander would need to be highly shock resistant and prevent tearing, leading to the use of a Kevlar weave fabric. However, due to the cost of such materials, the prototypes created and tested by our lab were modified. To keep mass down, the skeleton of the birdie was a mix of stainless steel and aluminum. The arms were made of extruded carbon fiber, with the chute being made of P1 parachute material. Though the P1 material is not tear resistant enough to survive impacts of ejecta faster than 1 km/s, it would be suitable for the low velocity test.

The skeleton was machined in house, while the chute was sewn by a volunteer parachute rigger. Two prototype, miniaturized chutes were sewn, one later becoming an actual prototype used for testing, Tinkerbell. Following the miniaturized test chutes, three full scale chutes were sewn at varying lengths.

An electronics package was developed for two birdies with the intention to control separation and deployment timing and altitude. The electronics consisted of a timer that initiates the burn of a "blast charge", or pack of black powder meant to separate the stages. The timer is started by the removal of a pull pin switch to ensure no ignition could occur in the helicopter.

4.2 BIRDIES

Individual reports on each birdie tested are outlined below. A consolidated table of characteristics for each tested birdie is below.

Table 4.7. Birdie Attribute Table

Birdie	Color	Mass (kg)	Surface Area (m^2)	Stowed Length (cm)	Electronics	Penetrator Pairing	Spring Force
Tinkerbell	Dark Green	0.13	0.44	61	No	Firefly	50 (2 springs)
Flora	Purple	0.23	1.9	107	No	Slim Jim	90 (3 springs)
Fauna	Bright Green	0.18	1.5	91	Yes/Off	Long John	90 (3 springs)
Merriweather	Orange	0.16	0.7	76	Yes/On	Stumpy	60 (2 springs)

4.2.1 *Birdie 1- Tinkerbell*

Tinkerbell, the smallest of the birdies to be tested, measured 76cm stowed, and had a total surface area of 0.44 m^2. The skeleton was made of stainless steel and aluminum, with a zero-porosity (0-P) nylon rip-stop parachute material used for the chute. This chute was sewn as a

prototype design to determine the process for sewing the three larger chutes. It was later decided to use Tinkerbell during the actual test for an additional data point.

Figure 4.3. Tinkerbell chute. A: Shown being stowed by hand. B: Chute open and upside down.

Tinkerbell was attached to the penetrator, Firefly, through a friction fit. The lander combination was dropped from roughly 760 meters above the surface of the glacier. As seen in Figure 4.4A, the chute failed to separate from the penetrator during the drop. This is believed to be due to the minimal mass, which didn't allow the lander combination to reach adequate velocity to create enough pressure to overcome the friction fit. When removed from the penetrator, as seen in Figure 4.4B, Tinkerbell's chute was slightly damaged. The carbon fiber rods ending the skeleton's arms poked through the ribbing material edging the parachute material. There was no further damage to the chute. The skeleton was undamaged by the impact.

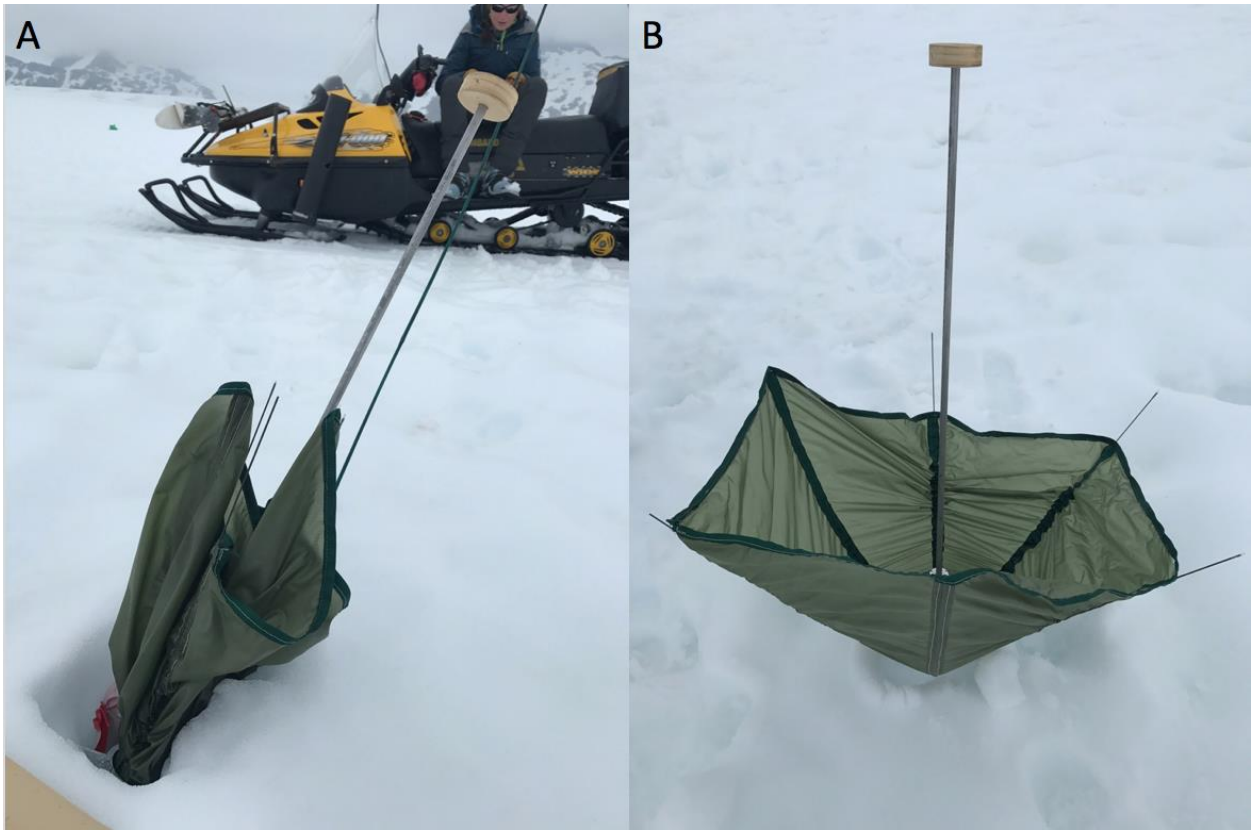

Figure 4.4. Tinkerbell impact. A: Untouched landing position. B: Chute when removed from penetrator.

4.2.2 *Birdie 2 – Flora*

Flora's skeleton is made of aluminum, stainless steel, and pultruded carbon fiber tubes. The carbon fiber tubes were filled with an extruded carbon fiber rod to act as a stabilizing core. The chute was sewn using two-porosity (2P) nylon rip-stop parachute material. The higher porosity material in comparison to Tinkerbell's chute did not affect any material properties and was used purely for price efficiency. The birdie had a total mass of 0.23kg.

Flora was paired with the penetrator Slim Jim. The system was the second combined system to be dropped from the helicopter, directly following the drop of Tinkerbell/Firefly. The drop from the helicopter went without issue until the separation of the birdie from the penetrator,

at which time the chute tore from the skeleton. This was due to thin nylon thread being used to attach the chute to the body in an attempt to lessen the possibility of binding the hinges of the skeleton. The birdie skeleton fell straight down after separation from the chute, with visual reference being kept from the helicopter until impact. The birdie skeleton was not affected by cross winds, as the following birdies were. This is most likely due to the lack of available surface area for wind to push against once the chute was stripped. Upon impact, as shown in Figure 4.6, the birdie skeleton was undamaged. Flora is estimated to have reached to highest velocity of the birdies due to the less of air resistance due to a lack of chute.

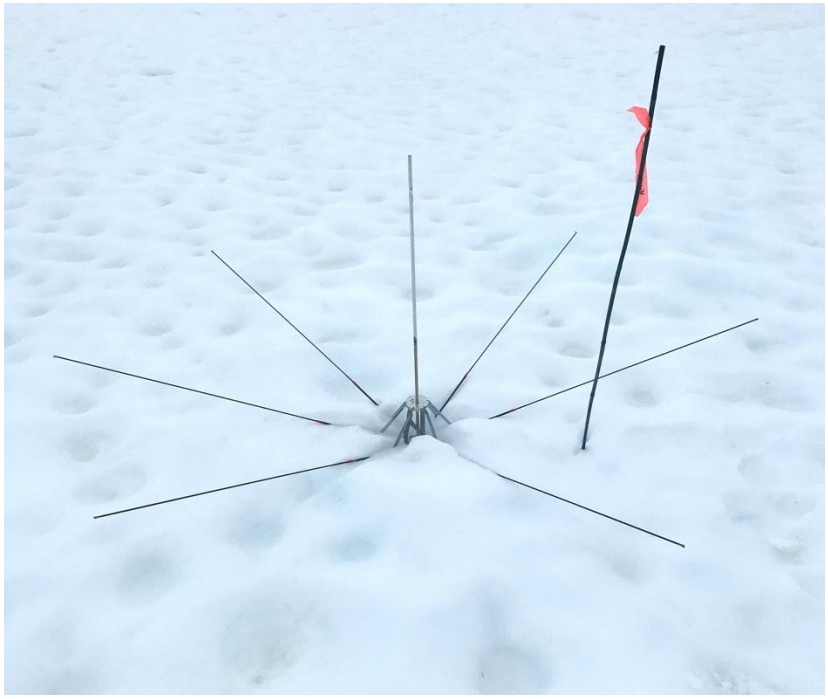

Figure 4.5. Flora undisturbed impact orientation. Due to minimal air resistance, the birdie fell straight down and impacted perpendicular to the glacier surface.

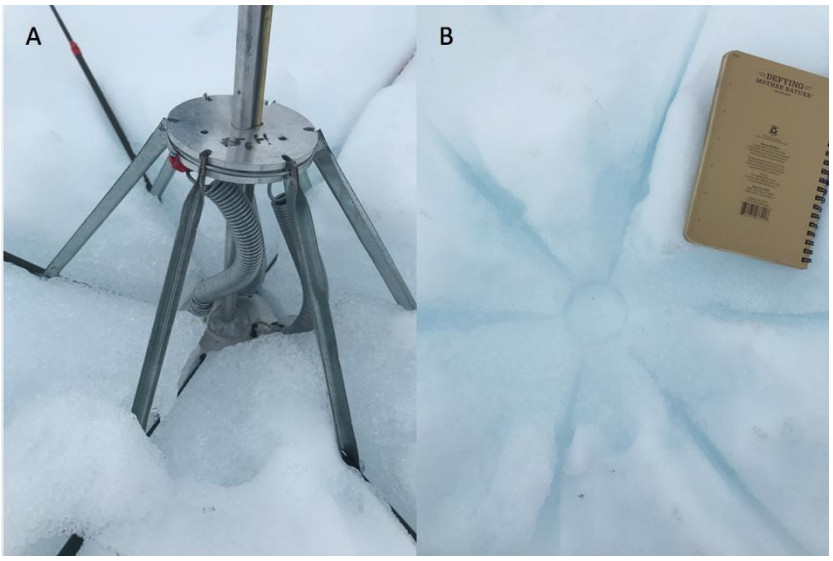

Figure 4.6. Close-up of Flora's Impact. A: Over compression of the springs caused the springs to bend. Otherwise no damage occurred to the skeleton. B: Snow imprint from Flora's skeleton. Based off small indentations, one arm bounced once before spreading to a larger angle than designed.

4.2.3 *Birdie 3 – Fauna*

The construction of Fauna was identical to that of Flora. The birdie had a total mass of 0.18 kg. This lander combination was the only set to test an electronic separation. The electronics, primarily a timer, ignited a black powder blast charge 12 seconds after being dropped from the helicopter. The blast charge removed a plastic cap from the opening of the penetrator, allowing air pressure to separate the birdie. This configuration allowed for the birdie to remain stowed for a longer amount of time than the other birdies.

To avoid the chute stripping from the skeleton as happened with Flora, 3mm parachute cord was used to tie the chute to the skeletons of both Fauna and Merriweather. With the additional ties, the chute remained attached during flight. Due to the design of the birdie to point into the path of most resistance, the birdie flew sideways when interacting with the wind during

flight. A distinctive scallop shaped flight path tracing the wind patterns occurred when the birdie entered the two separate wind bands, as illustrated in Figure 4.9.

Figure 4.7. Full configuration of Fauna and Long John.

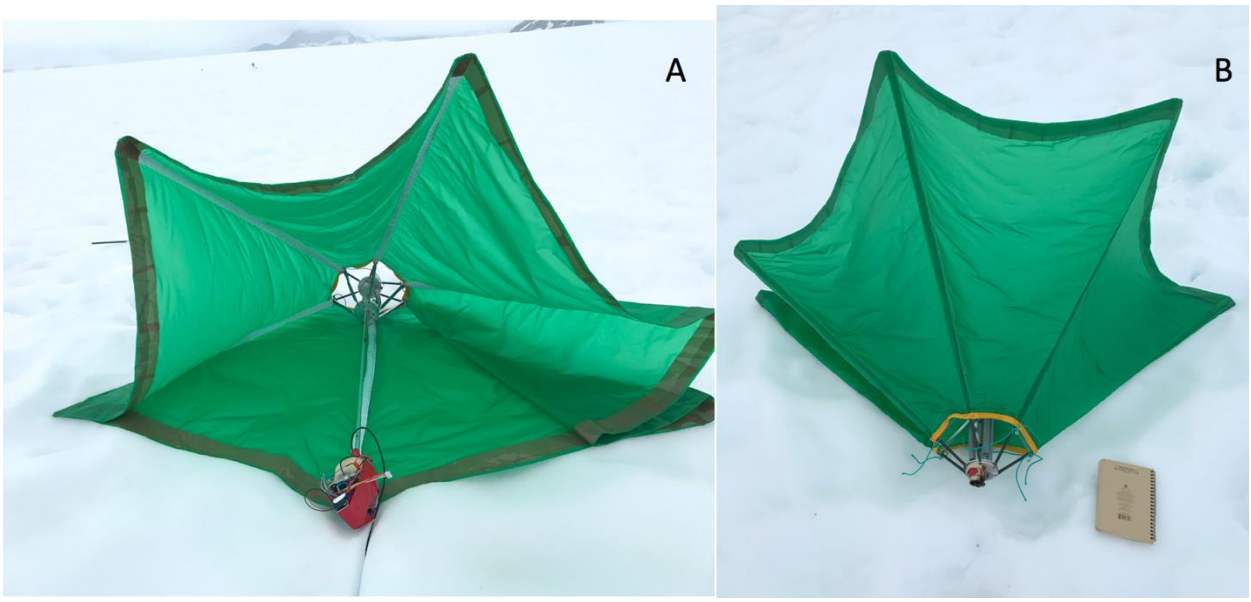

Figure 4.8. Fauna landing position. A: Viewed from the south. B: Viewed from the north.

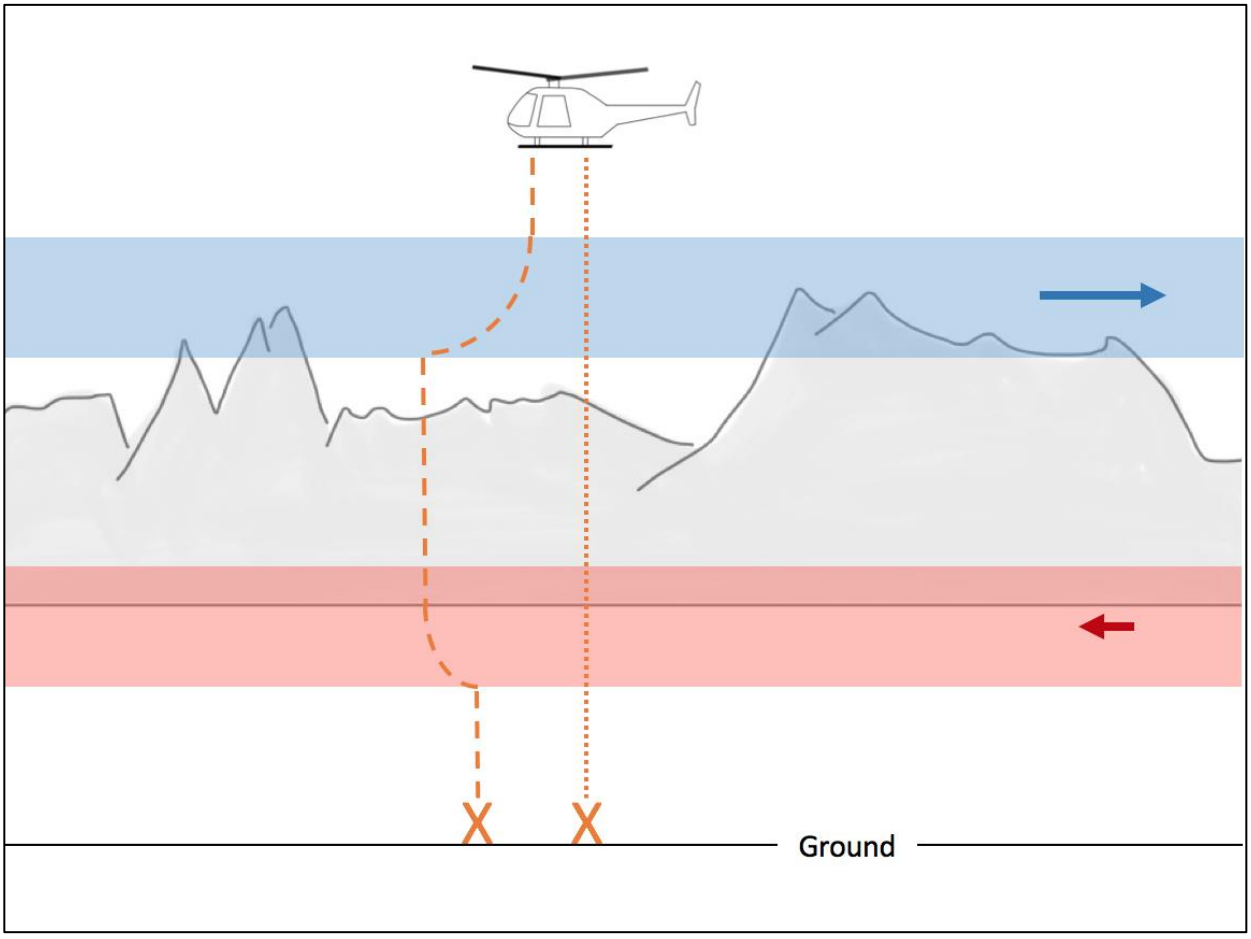

Figure 4.9. Trajectory path of birdies through wind bands. Colored bands show wind bands, corresponding color arrow shows wind direction and magnitude. Dotted line shows trajectory without wind interaction. Dashed line shows trajectory of birdie, steering into oncoming wind.

4.2.4 *Birdie 4 – Merriweather*

The construction was identical to that of Flora. The birdie had a total mass of 0.16kg. This lander configuration was originally set up to run an electronic separation payload identical to that of Fauna, however a friction separation was decided upon flight preparation to avoid multiple deployment failures if the electronics failed. Due to the mass differences between the highly massive penetrator and relatively light birdie, separation occurred almost instantaneously upon release from the helicopter. Merriweather also contained only two springs, in comparison to the other large birdies containing three. These two factors led to Merriweather only partially deploying during flight. Even with partial deployment, Merriweather displayed the same scalloping descent while encountering the wind bands, though to a less extreme degree than Fauna.

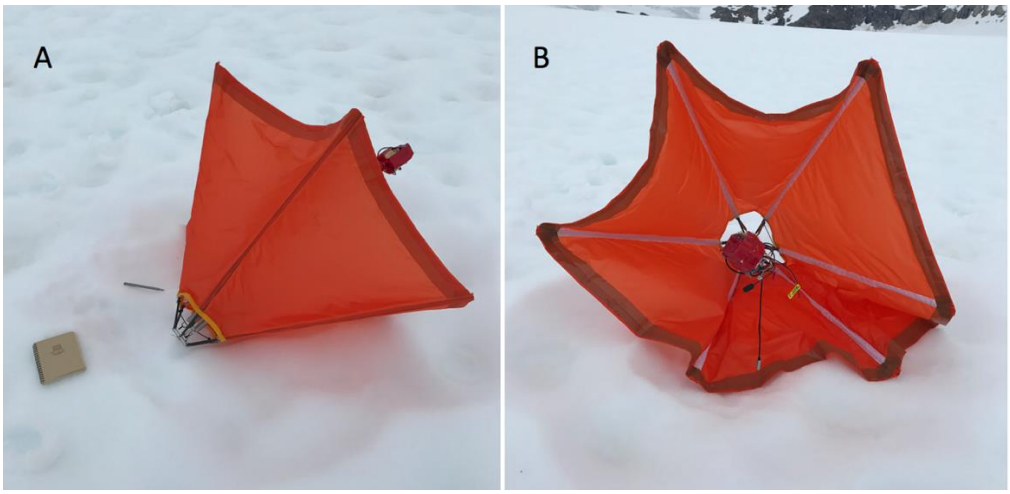

Figure 4.10. Merriweather impact viewed from east (A) and south (B).

4.3 Results and Future Work

Overall, each birdie both failed and succeeded in different ways. Though Flora's chute stripped, it is now known how the birdies would react without air resistance during flight. Fauna separated when the timer was set, though it was decided an altitude based deployment system would allow for better chute interaction with possible plumes. Merriweather exemplified the need for strong resistance to ejecta, in this case represented by air resistance.

The most pressing result of this field test of the second stage was determining the flight stability of the second stage after deployment, as well as the means of deployment. The design avoided tumbling during deployment and flight, but failed to open fully in face of high velocity. A chute deployment with higher spring-force may improve this problem. For the deployment technique, the timer worked suitably well, though the blast charge must be replaced with another release mechanism.

Future designs of the birdies will focus on more robust skeletons, as well as deployment electronics. For birdies truly intended for interaction with ice plumes, Kevlar chutes would be needed instead of nylon. The carbon fiber skeletons, though light, proved to brittle to sustain impacts with high velocity ejecta. A stronger alternative would be needed.

Chapter 5. PROPOSED RESEARCH

5.1 Alaskan Glacier Test

A second, future trip to the Juneau Icefield is in planning for August 2018. This test will occur on the Gilkey Glacier, in an attempt to impact ice instead of seasonal snowpack. This will also be

done with rocket propulsion instead of static drops from a helicopter, with the intent to reach higher velocities. Sugar motors are being created, which in contrast to the regular rocket motors used contain no ammonium perchlorate. This chemical is toxic and will be avoided to not allowed contamination of the glacier.

5.2 Alaskan Sea Ice Test

A further impact test is planned for March 2018 to Barrow, AK to impact sea ice at high velocities. This test is intended to create ice plumes in a more controllable situation than on the Juneau Icefield. Additionally, sea ice is less dense than blue glacier ice, giving an additional data point of substrate relative hardness.

5.3 Birdie Development

Additional to the improvements mentioned in section 4.3, further development of the second stage is being conducted. An energy absorption material (Truitt 2016) modified and contained within the second stage to protect electronics at high velocity impacts is currently being developed. The design will be tested with small scale impacts similar to the initial ice penetrator laboratory testing.

5.4 Biological Capture and Detection

Further testing of the "biology shots" will be continued, with a focus on microbial damage within impact zones. Caution will be taken to minimize contamination during these experiments.

An additional test at larger scale will be conducted in Barrow, AK during the planned sea-ice field test. Trapped algae within the sea ice will be analyzed optically to determine the effect of a supersonic impact in the surrounding ice.

BIBLIOGRAPHY

Collinson, G. "Planetary Penetrators - The Vanguard for the Future Exploration of the Solar System." *Journal of the British Interplanetary Society* 61 (2008): 198-202. Web.

Gowen, R. A. "Penetrators for in Situ Subsurface Investigations of Europa." *Elsevier* 48.4 (2011): 725-42. *Advances in Space Research*. Pergamon, 19 June 2010. Web. 27 Dec. 2017.

Hertzberg, A., A. P. Bruckner, and D. W. Bogdanoff. "Ram Accelerator - A New Chemical Method for Accelerating Projectilesto Ultrahigh Velocities." *AIAA Journal* 26.2 (1988): 195-203. Web.

Mastrapa, R. M. E., H. Glanzberg, J. N. Head, H. J. Melosh, and W. L. Nicholson. "Survival of Bacteria Exposed to Extreme Acceleration: Implications for Panspermia." *Earth and Planetary Science Letters*. Elsevier, 14 June 2001. Web. 28 Dec. 2017.

Mykytczuk, Nadia. "Bacterial Growth at −15 °C; Molecular Insights from the Permafrost Bacterium Planococcus Halocryophilus Or1." *Medscape Log In*. The ISME Journal, 07 Feb. 2013. Web. 28 Dec. 2017.

Osinski, Gordon R., and Elisabetta Pierazzo. *Impact Cratering: Processes and Products*. Hoboken, NJ: John Wiley & Sons, 2013. Print.

Paranicas, C., J. M. Ratliff, B. H. Mauk, C. Cohen, and R. E. Johnson. "The Ion Environment near Europa and Its Role in Surface Energetics." *Geophysical Research Letters* 29.5 (2002): n. pag. Web.

Robinson, Tessa, Robert M. Winglee, and Carl Knowlen. *Europa Kinetic Ice Penetrator System for Hyper Velocity Instrument Deposition*. Thesis. University of Washington, 2017. N.d. N.p.: n.p., n.d. Print.

Spencer, J. R., L. K. Tamppari, T. Z. Martin, and L. D. Travis. "Emperatures on Europa from Galileo Photopolarimeter-Radiometer: Nighttime Thermal Anomalies." *Science*284.5419 (1988): 1514-516. Web.

Truitt, Chad. *Planetary Penetrators for Sample Return Missions*. Thesis. University of Washington, 2016. N.p.: n.p., n.d. Print.

Winglee, R. M., T. Robinson, M. Danner, and J. Koch. "Cryo-braking Using Penetrators for Enhanced Capabilities for the Potential Landing of Payloads on Icy Solar System Objects." *Acta Astronautica* 144 (2018): 136-46. Web.

Winglee, R.m., C. Truitt, and R. Shibata. "High Velocity Penetrators Used a Potential Means for Attaining Core Sample for Airless Solar System Objects." *Acta Astronautica* 137 (2017): 274-86. Web.

Wunnemann, K., and B. A. Ivanov. "Numerical Modelling of the Impact Crater Depth–diameter Dependence in an Acoustically Fluidized Target." *Planetary and Space Science*. Pergamon, 04 Oct. 2003. Web. 28 Dec. 2017.

APPENDIX A

Past and Pending Missions to/near Europa or Icy Bodies:

Mission	Launch Year	Decommissioned
Pioneer 10 & 11	1973	--
Galileo	1989	--
Galileo Europa Mission (GEM)	1997	--
Rosetta	2004	2014, Impact Philae
Juno	2011	--
Europa Clipper (Orbiter & Lander) **	2020's	--

**Denotes future/pending mission

VITA

[A short bio of the author is required for a Ph.D. dissertation at the University of Washington. The vita section does not go into the Table of Contents. The formatting style follows the text of the dissertation.]